iScience

CellPress

Article

Leptosphaeria maculans Effector Protein AvrLm1 Modulates Plant Immunity by Enhancing MAP Kinase 9 Phosphorylation

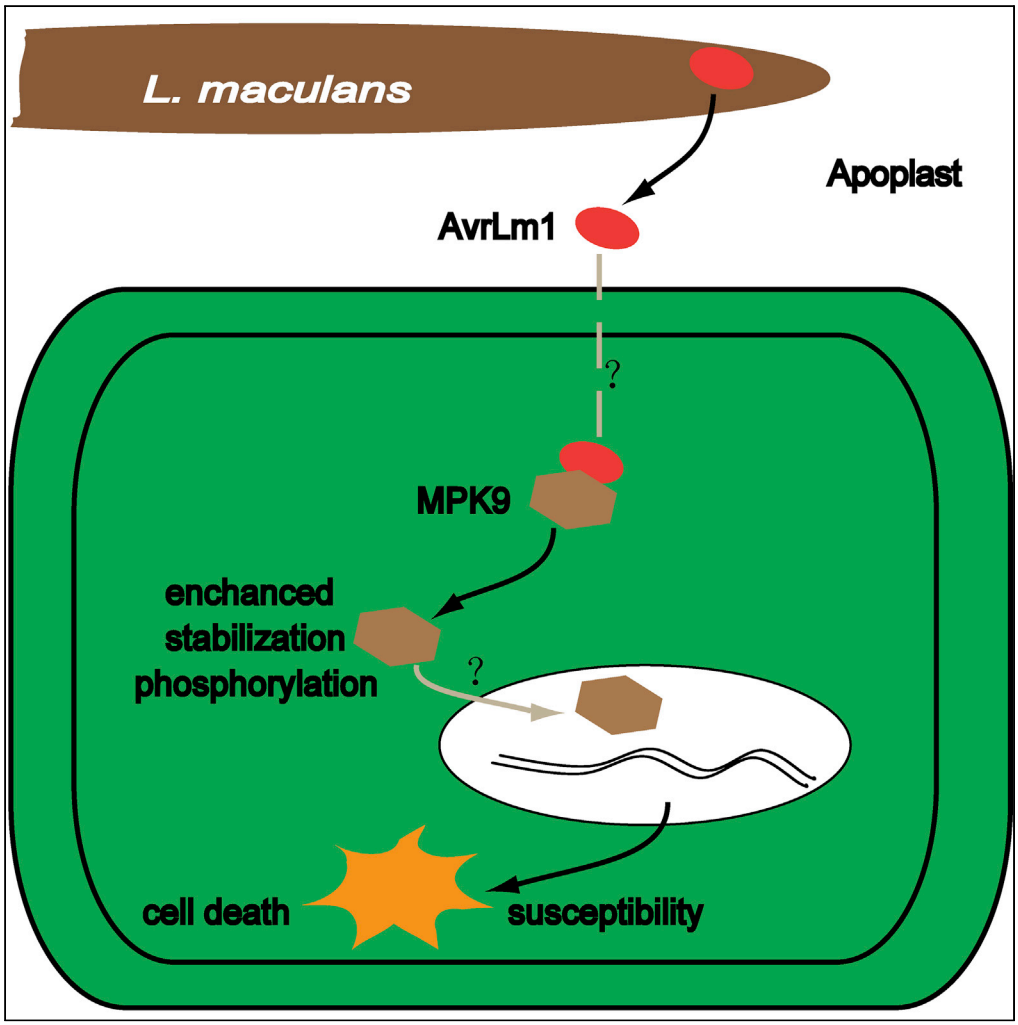

Lisong Ma, Mohammad Djavaheri, Haiyan Wang, ..., Elena Beynon, Gordon Gropp, M. Hossein Borhan

hossein.borhan@agr.gc.ca

HIGHLIGHTS

Leptosphaeria maculans effector AvrLm1 interacts with the *Brassica napus* MPK9 (BnMPK9)

AvrLm1 increases the accumulation and enhances the phosphorylation of BnMPK9

AvrLm1 enhances BnMPK9-dependent cell death in *Nicotiana benthamiana*

Stable expression of *BnMPK9* in *B. napus* facilitates *L. maculans* infection

Ma et al., iScience 3, 177–191
May 25, 2018 https://doi.org/10.1016/j.isci.2018.04.015

iScience

CellPress

Article

Leptosphaeria maculans Effector Protein AvrLm1 Modulates Plant Immunity by Enhancing MAP Kinase 9 Phosphorylation

Lisong Ma,[1] Mohammad Djavaheri,[1] Haiyan Wang,[2] Nicholas J. Larkan,[1,3] Parham Haddadi,[1] Elena Beynon,[1] Gordon Gropp,[1] and M. Hossein Borhan[1,4,*]

SUMMARY

***Leptosphaeria maculans*, the causal agent of blackleg disease in canola (*Brassica napus*), secretes an array of effectors into the host to overcome host defense. Here we present evidence that the *L. maculans* effector protein AvrLm1 functions as a virulence factor by interacting with the *B. napus* mitogen-activated protein (MAP) kinase 9 (BnMPK9), resulting in increased accumulation and enhanced phosphorylation of the host protein. Transient expression of *BnMPK9* in *Nicotiana benthamiana* induces cell death, and this phenotype is enhanced in the presence of AvrLm1, suggesting that induction of cell death due to enhanced accumulation and phosphorylation of BnMPK9 by AvrLm1 supports the initiation of necrotrophic phase of *L. maculans* infection. Stable expression of *BnMPK9* in *B. napus* perturbs hormone signaling, notably salicylic acid response genes, to facilitate *L. maculans* infection. Our findings provide evidence that a MAP kinase is directly targeted by a fungal effector to modulate plant immunity.**

INTRODUCTION

Fungal pathogens of crop plants cause significant yield losses and affect global food security, particularly in the face of increased demand due to a growing world population (Fisher et al., 2012). Diverse lifestyle, genome plasticity and evolution, prolific reproduction, and longevity of spores under harsh environment impede the efficient control of fungal diseases. Like bacterial and oomycete plant pathogens, fungi also secrete small proteins, known as effectors, which counter plant defense and modulate plant physiology to promote pathogen growth and reproduction (Presti et al., 2015; Stergiopoulos and de Wit, 2009). Accumulating evidences show that the secreted effectors are key players in suppressing pathogen-associated molecular patterns (PAMPs)-triggered immunity (PTI) induced upon fungal recognition by plant (Presti et al., 2015). As an example, the lysine motif (LysM) effector ECP6 secreted by the tomato pathogen *Cladosporium fulvum* suppresses chitin triggered immunity. ECP6 binds chitin via the intramolecular chitin-binding groove formed by the LysM domains, resulting in the sequestering of chitin released from the cell walls of invading hyphae (de Jonge et al., 2010; Sánchez-Vallet et al., 2013). Plants, on the other hand, have evolved disease resistance (*R*) genes encoding receptor proteins that detect and respond to pathogen effector proteins, leading to the activation of effector-triggered immunity (ETI) (Jones and Dangl, 2006). Effectors that trigger ETI are referred to as avirulence (Avr) genes. Discovery of the host targets of effectors is essential for our understanding of effector activity and molecular mechanisms of plant defense (Win et al., 2012). There are many examples of plant proteins that are targeted by bacterial effectors secreted by the type III secretion system (Block and Alfano, 2011; Deslandes and Rivas, 2012). However, despite the economic importance of diseases caused by the fungal plant pathogens, for most fungal effectors, the host targets and underlying molecular mechanisms remain unknown.

Mitogen-activated protein (MAP) kinase cascades are highly conserved signaling modules in eukaryotes and have a central role in plant immunity against pathogen attack (Meng and Zhang, 2013; Pitzschke et al., 2009). A MAP kinase cascade is commonly composed of three types of kinases including a MAP kinase kinase kinase (MAPKKK), a MAP kinase kinase (MKK), and a MAP kinase (MPK). In *Arabidopsis*, pathogen-responsive MPK signaling has been reported to be involved in both PTI and ETI, in which the best characterized MPKs are MPK3, MPK4, and MPK6 (Asai et al., 2002; Rasmussen et al., 2012). PAMPs, such as flg22 (a conserved 22-amino acid flagellin peptide) and elf18 (elongation factor-Tu peptide), activate the kinase signaling cascades involving MPK3, MPK4, and MPK6 (Felix et al., 1999; Gao et al., 2008;

[1]Saskatoon Research and Development Centre, Agriculture and Agri-Food Canada, 107 Science Place, Saskatoon, SK S7N 0X2, Canada

[2]Center of Plant Disease and Plant Pests of Hebei Province, College of Plant Protection, Hebei Agricultural University, Baoding 071001, China

[3]Armatus Genetics Inc., Saskatoon, SK S7J 4M2, Canada

[4]Lead Contact

*Correspondence: hossein.borhan@agr.gc.ca

https://doi.org/10.1016/j.isci.2018.04.015

Zipfel et al., 2006). In contrast, plant pathogens have evolved mechanisms to target the MPK signaling pathways to enhance plant susceptibility. For example, *Pseudomonas syringae* HopAI1 targets MPK3 and MPK6 and inactivates their kinase function to suppress plant defense responses (Zhang et al., 2007). *P. syringae* HopF2 targets MKK5 and can inactivate MKK5 via ADP-ribosylation of the C terminus of MKK5 *in vitro* (Wang et al., 2010). AvrB is a *P. syringae* effector that interacts with MPK4 to perturb hormone signaling and promote infection (Cui et al., 2010). *Phytophthora infestans* RXLR effector PexRD2 as a virulence factor interacts with the kinase domain of the host MAPKKKε to suppress MAPKKKε-dependent phosphorylation of MPKs to modulate plant immunity (King et al., 2014). These findings highlight the importance of MPK pathways in plant immunity and as targets of bacterial and oomycete pathogen effectors. However, to date no MAPKs have been identified as targets of effectors from fungal plant pathogens.

Plant MPKs can be classified into four groups (A, B, C, D) based on the conserved amino acid sequences of the TxY motif present in the activation loop of MPKs (Ichimura et al., 2002). Among the best studied MPKs, MPK3 and MPK6 are in group A and MPK4 belongs to group B. However, MPK9 belongs to the D group with the plant-specific TDY phosphorylation motif and is distinct from the A, B, and C groups. In *Arabidopsis*, previous studies have reported that AtMPK9, together with AtMPK12, is involved in stomatal closure (Lee et al., 2016). Both abscisic acid (ABA)- and methyl jasmonate-induced stomatal closure are impaired in *Arabidopsis* double *mpk9/mpk12* mutants, but not in *mpk9* or *mpk12* single mutants, indicating a functional redundancy (Jammes et al., 2009; Khokon et al., 2015). The *mpk9/mpk12* double mutant is highly susceptible to *P. syringae* pv. *tomato* (*Pst*) DC3000 infection (Jammes et al., 2011). However, Montillet et al. (2013) reported that ABA signaling, including open stomata 1 (OST1) protein kinase, AtMPK9, or AtMPK12, plays a limited role in response to *Pst* early infection. This is based on the observations that there is no difference between double *mpk9/mpk12* mutants and wild-type *Arabidopsis* Col in response to flg22-induced stomatal closure and expression of ABA-specific marker genes is not affected by *Pst* treatment (Montillet et al., 2013). Thus it is unclear whether MPK9 acts in ABA-mediated guard cell immune signaling in response to biotic stresses. More recently, a study by Nagy et al. (2015) revealed that AtMPK9 is activated through intramolecular autophosphorylation independent of any upstream MAPKKs, which is similar to MAPKK-independent activation mechanisms reported for the mammalian atypical MAPKs, such as extracellular signal-regulated kinase (ERK)7/8 (Klevernic et al., 2006; Nagy et al., 2015).

Leptosphaeria maculans, the fungal agent of blackleg disease (phoma stem canker), causes major yield loss on *Brassica napus* (canola/rapeseed) crops worldwide (West et al., 2001). During infection it remains extracellular and exhibits a range of modes of infection from biotrophy to necrotrophy on *Brassica* hosts. Genome-wide transcriptomic analyses in the *B. napus-L. maculans* pathosystem revealed that the majority of known and predicted effectors had no expression during *in vitro* culture but were highly up-regulated during infection, supporting their roles as virulence factors (Haddadi et al., 2016). Resistance against *L. maculans* at the cotyledon stage is race specific. So far, 19 race-specific resistance (*R*) genes have been reported from *Brassica* species (Larkan et al., 2016), but only two *R* genes, *LepR3* and *Rlm2*, have been cloned, both encoding membrane-localized receptor-like proteins (RLPs) (Larkan et al., 2013, 2015). LepR3 perceives *L. maculans* AvrLm1 and triggers *Brassica* defense, leading to hypersensitive response (HR) at the site of infection (Larkan et al., 2013). Transient expression of both *LepR3* and *AvrLm1* induces HR in *Nicotiana benthamiana* leaves, and SOBIR1 and BAK1 receptor-like kinases (RLK), two components of LepR3 complex, are required for the perception of AvrLm1 (Ma and Borhan, 2015). To date, seven *Avr* genes (*AvrLm1*, *2*, *3*, *4–7*, *5–9*, *6*, and *11*) have been cloned from *L. maculans*, all encoding cysteine-rich proteins, except for AvrLm1, which contains only one cysteine residue (Gout et al., 2006). Cysteine enrichment is a feature found in most of the effectors of apoplastic fungi such as *L. maculans* and is believed to protect the effector protein, by formation of disulfide bonds, from plant proteases released into the apoplastic space during pathogen invasion (van den Burg et al., 2003). Lack of cysteine enrichment in the AvrLm1 protein could indicate that AvrLm1 is translocated inside the plant host cells. Given that LepR3 is a cell surface receptor, recognition of AvrLm1 by LepR3 likely occurs in the apoplast (Gout et al., 2006; Larkan et al., 2013; Ma and Borhan, 2015). However, it is still possible that AvrLm1 is translocated inside the plant cells to modulate host immunity. Owing to technical challenges, host cellular location for a vast majority of effector proteins of fungal and oomycete plant pathogens has not been determined and localization of pathogen effectors in the host plant is often inferred from their structure and their plant target proteins.

Although *AvrLm1* was cloned a decade ago, the host target and molecular mechanism underlying AvrLm1 virulence have remained unknown. In this study, we report the identification of MPK 9 as a novel target of *L. maculans* effector AvrLm1. Stable expression of *BnMPK9* in *B. napus* enhances the growth of *L. maculans*

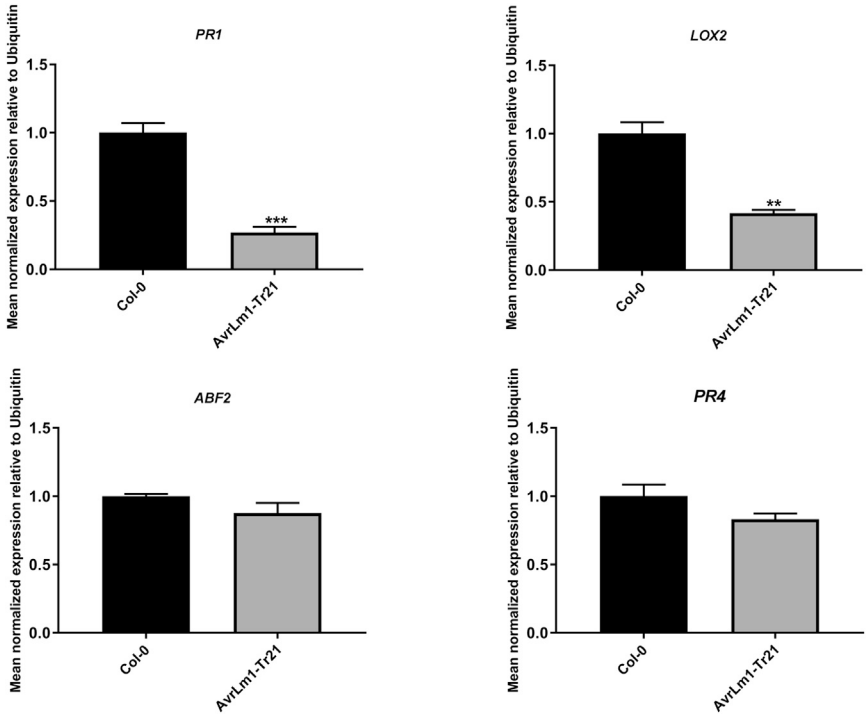

Figure 1. Relative Expression of Salicylic Acid (SA), Ethylene (ET), Jasmonic Acid (JA) and Abscisic Acid (ABA) Marker Genes in AvrLm1-Expressing *Arabidopsis* Lines

Leaves of 4-week-old plants were collected for RNA extraction. Expressions of *Arabidopsis* defense marker genes including *PR1*, *LOX2*, *ABF2*, and *PR4* were determined by quantitative reverse-transcriptase polymerase chain reaction and normalized to *Arabidopsis* ubiquitin gene. Values represent means ± standard error (SE) from three independent experiments. ** and *** represent the significant differences ($p < 0.01$, and $p < 0.001$, respectively, a two-tailed Student's *t* test).

by suppressing the salicylic acid (SA) pathway, suggesting that BnMPK9 negatively regulates plant defense. Our findings indicate that AvrLm1 as a virulence factor functions by stabilizing BnMPK9 and inducing its phosphorylation, leading to enhanced cell death and plant susceptibility to the hemibiotrophic pathogen *L. maculans*.

RESULTS

AvrLm1 as a Virulence Factor Modulates Plant Hormone Signaling

Effectors contribute to fungal virulence by protection of fungal structures and modulation of host metabolism. Comparison of near-isogenic *L. maculans* isolates with and without the effector AvrLm1 suggested that isolates carrying *AvrLm1* were more aggressive on susceptible *B. napus* cultivars (Huang et al., 2009). To further examine the virulence function of AvrLm1, we generated transgenic *Arabidopsis* Columbia-0 (Col-0) lines carrying *AvrLm1* in which expression of the full-length *AvrLm1* gene was driven by the constitutive CaMV 35S promoter. A homozygous single-insertion line was generated (Col-*AvrLm1*), and expression of *AvrLm1* was confirmed by quantitative reverse-transcriptase polymerase chain reaction (qRT-PCR) (See Figure S1). Expression of SA, jasmonic acid (JA), ethylene (ET), and ABA signaling response marker genes (*PR1, LOX-2, PR4, and ABF2)* in Col-*AvrLm1* and Col-0 plants were compared. Expressions of *PR1* and *LOX2* were significantly decreased in Col-*AvrLm1*, whereas expressions of *ABF2* and *PR4* were the same as in Col-0, indicating that AvrLm1 suppress SA and JA signaling but does not affect the ABA and ET pathways (Figure 1). Col-*AvrLm1* plants were challenged with the bacterial pathogen *Pst* DC3000. Col-0 was also inoculated with *Pst*-DC3000 as a control. As shown in Figure 2, Col-*AvrLm1* showed enhanced disease symptoms (severe chlorosis) and higher bacterial growth compared with the Col-0 control. These findings indicate that AvrLm1 functions as a virulence factor by suppressing plant defense.

AvrLm1 Is Secreted into the Apoplast of *Brassica* upon *L. maculans* Infection

L. maculans resides in the plant extracellular space during *Brassica* infection. To monitor AvrLm1 during *L. maculans* infection, *AvrLm1* driven by its native promoter was tagged with the fluorescent protein

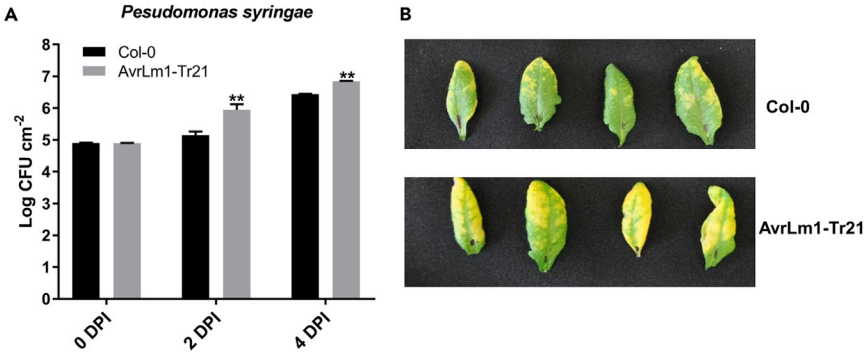

Figure 2. *AvrLm1*-Expressing *Arabidopsis* Is More Susceptible to *Pseudomonas syringae*

(A) Bioassay was performed on Col-0 and one Col-0 35S::Δsp*AvrLm1* (AvrLm1-Tr21) transformant. Bacterial growth of *P. syringae* was scored at 0, 2, and 4 dpi. Bars indicate standard deviation of eight replicates; ** indicates significant difference between the wild-type Col-0 and the AvrLm1-Tr21 in a two-tailed Student's *t* test ($p = 0.01$).

(B) Photographs were taken from representative leaves at 4 dpi.

mCherry and transferred to *L. maculans* isolate 3R11 (3R11:*AvrLm1-mCherry*). An additional transgenic isolate carrying the fluorescent gene YFP driven by a fungal constitutive promoter was generated to serve as a control. To ensure that addition of mCherry tag to AvrLm1 did not disrupt its Avr function (being recognized by LepR3) or the overall fitness of 3R11 isolate, the 3R11:*AvrLm1-mCherry* was inoculated on the susceptible *B. napus* cultivar Topas DH16516 and the Topas:*LepR3* transgenic line NLA8-2 (Larkan et al., 2013). The 3R11:*AvrLm1-mCherry* was virulent on Topas DH16516 (see Figure S2). As anticipated, the transgenic strain 3R11:*AvrLm1-mCherry* was avirulent on the *LepR3*-transformed NLA8-2 line, confirming that addition of mCherry tag did not interfere with the function of AvrLm1 (Figure S2). Subsequently, 3R11:*AvrLm1-mCherry* was inoculated on the host Topas DH16516 plants for the localization study. Infected cotyledons of Topas DH16516 were examined by confocal microscopy, and red fluorescent signals of the tagged AvrLm1 were detected along the cell wall of the hyphae. Intense focal fluorescent spots were observed where intercellular hyphae were in contact with the host mesophyll cells. In contrast, yellow fluorescent signals in the control 3R11-YFP were more uniformly observed throughout the fungal hyphae (Figure 3). We were not able to detect AvrLm1-mCherry inside the cell or apoplastic space of the host infected tissue. However, accumulation of mCherry signals along the hyphal cell wall and particularly focal accumulation where hyphae were in the vicinity of host cells could be an indication of localized AvrLm1 secretion into the apoplast or accumulation within the cytoplasm of the host plant cells.

To further investigate if AvrLm1-mCherry protein accumulates in the apoplast, we extracted the apoplastic fluids from *L. maculans*-infected cotyledons at 4 days post-inoculation (dpi). Apoplastic fluid was probed with anti-mCherry antibody, and AvrLm1-mCherry fusion protein was detected from the apoplastic fluids isolated from the infected plants (Figure S3). In conclusion, the localization of AvrLm1-mCherry on the surface of the fungal hyphae and detection of secreted AvrLm1-mCherry proteins in the apoplastic fluids indicate that AvrLm1-mCherry is very likely secreted into the apoplast.

AvrLm1 Physically Associates with BnMPK9

To investigate the molecular mechanism underlying the AvrLm1 virulence function, yeast two-hybrid screening was performed using AvrLm1 without signal peptide (ΔspAvrLm1) as a bait against a prey cDNA library prepared from young *Arabidopsis* seedlings. Four AvrLm1-interacting candidate proteins from *Arabidopsis* were identified including EBF1 (EIN3-binding F box protein 1), MPK17, MPK9, and T21P5.2 (hypothetical protein) (see Table S1). To validate the interaction for the candidate proteins, ΔspAvrLm1 was used as the bait against each of the protein product of *Arabidopsis AtEBF1*, *AtMPK17*, *AtMPK9*, and *AtT21P5.2* with full-length open reading frames as the respective preys. Among the four candidates only full-length AtMPK9 (AT3G18040) was validated as interacting with AvrLm1 (Figure S4). BLAST search against the genome of *B. napus* Darmor-*bzh* (Chalhoub et al., 2014) identified two *Brassica* homologs of *AtMPK9*, BnaA05g22170D and BnaCnng17720D, residing in the A and C genomes of *B. napus*, respectively. Protein sequence alignment (Figure S5) identified that both shared the same level of homology with AtMPK9. Therefore only one gene, BnaCnng17720D (hereafter referred to as BnMPK9), was chosen for further analysis. Interaction between AvrLm1 and BnMPK9 was confirmed by yeast two-hybrid assay

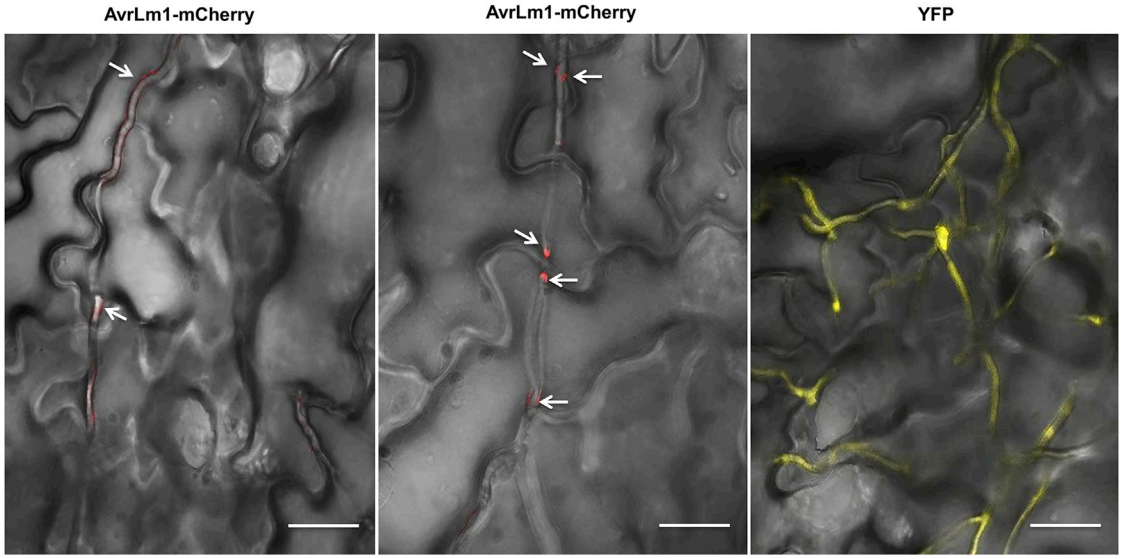

Figure 3. Localization of AvrLm1 upon *L. maculans* Infection of *Brassica*

One-week-old Topas DH16516 seedlings were inoculated with spore suspension and cotyledons were used for microscopic observation at 4 days post-inoculation. Transgenic *L. maculans* 3R11 carrying *AvrLm1-mCherry*, whose expression was driven by the native *AvrLm1* promoter or carrying *YFP* under constitutive promoter, was visualized using confocal microscopy. Arrows indicate the local accumulation of AvrLm1-mCherry and secreted AvrLm1-mCherry aligning the fungal cell wall. No mCherry signal could be detected within the mycelium of *L. maculans* 3R11 expressing only *YFP*. Scale bars represent 25 μm.

(Figure 4A). We next confirmed this interaction with bimolecular fluorescence complementation (BiFC) *in planta*. To generate the BiFC constructs, pENTR/Zeo:*BnMPK9* and pENTR/Zeo:*ΔspAvrLm1* were recombined into the binary vectors pDEST-GW-VYCE and pDEST-GW-VYNE. BiFC assay was performed by transiently co-expressing *ΔspAvrLm1-VYNE* or *BnMPK9-VYNE* with *BnMPK9-VYCE* in *N. benthamiana* leaves. As shown in Figure 4B, a strong yellow fluorescent signal was observed in cells co-expressing *AvrLm1-VYCE* and *BnMPK9-VYNE*, but not with the negative control (*BnMPK9VYNE* and *BnMPK9VYCE*). To further validate this association *in vivo*, the co-immunoprecipitation assay was performed upon transient expression of *HA-BnMPK9* and *AvrLm1-GFP* constructs in *N. benthamiana*. Hemagglutinin (HA)-tagged BnMPK9 co-immunoprecipitated with green fluorescence protein (GFP)-tagged AvrLm1, and *vice versa* (Figures 4C and S6). Taken together, these observations support that BnMPK9 is the host target for AvrLm1.

AvrLm1 Specifically Interacts with BnMPK9 and Its Small N-Terminal Region Is Dispensable for the Interaction

It has been reported that *Arabidopsis* MPK9 and MPK12 positively regulate ABA, SA, and MeJA signaling in *Arabidopsis* (Jammes et al., 2009; Khokon et al., 2017) and MPK9 and MPK12 are functionally redundant. Two other *Arabidopsis* MPKs, AtMPK3 and AtMPK6, are well known to be involved in plant immunity (Asai et al., 2002). To assess whether AvrLm1 specifically interacts with BnMPK9, we tested the interaction of AvrLm1 with either AtMPK12 or BnMPK3 in yeast two-hybrid (Y2H) assay. Neither AtMPK12 nor BnMPK3 interacted with AvrLm1, confirming the specificity of interaction between AvrLm1 and BnMPK9 (Figure S7).

To define which region of AvrLm1 is required for the interaction with BnMPK9, three N-terminally and one C-terminally truncated AvrLm1 proteins were generated based on the predicted AvrLm1 secondary structure (Ma and Borhan, 2015). Four variants were constructed: AvrLm1-Δ40, AvrLm1-Δ73, AvrLm1-Δ108, and CTΔ14. Only AvrLm1-Δ40 interacted with BnMPK9 (Figure 5A), indicating that a small (40-amino acid [aa]) N-terminal region of AvrLm1 is not required for the interaction but the remaining region of AvrLm1 is indispensable for its interaction with MPK9. To further define the region of BnMPK9 that is required to interact with AvrLm1, we generated three truncations of *BnMPK9* that were used for Y2H with AvrLm1. One of them carrying a small N-terminal deletion region (95 aa) enabled the growth of yeast on selective plates, indicating that deletion of up to 95 N-terminal amino acid from the BnMPK9 protein does not disrupt its interaction with AvrLm1 (Figure 5B).

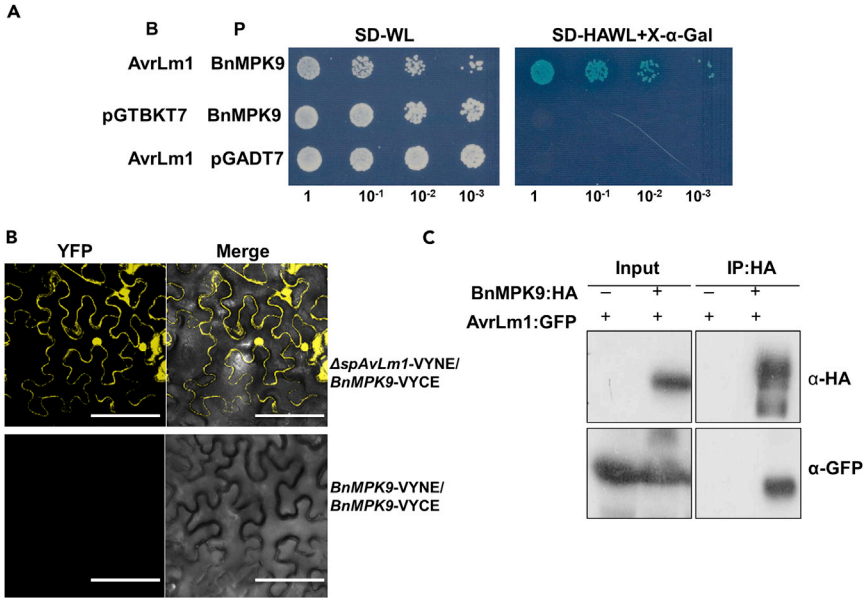

Figure 4. AvrLm1 Associates with BnMPK9

(A) Interaction of AvrLm1 and BnMPK9 was detected by Y2H. Yeasts expressing the indicated combinations of bait (B) and prey (P) were spotted on the synthetic dropout medium without leucine and tryptophan (SD-WL) and SD medium without leucine, tryptophan, histidine, and adenine supplemented with X-α-Gal and Aureobasidin A (SD-HAWL + X-α-Gal). Only those co-expressing *AvrLm1* and *BnMPK9* grew on SD-HAWL plates and developed blue coloration, indicative of an interaction between both proteins.

(B) BiFC confirmed the interaction between AvrLm1 and BnMPK9. VYCE-fused *BnMPK9* and VYNE-fused *AvrLm1* were transiently co-expressed in *N. benthamiana*. Co-infiltration of VYNE-fused *BnMPK9* and VYCE-fused *BnMPK9* was used as negative control. Yellow florescent protein (YFP) signal was visualized by confocal microscopy. Yellow fluorescence confirms protein-protein interaction due to complementation of the split YFP protein.

(C) Co-immunoprecipitation of AvrLm1 and BnMPK9 from the total plant protein extracts. GFP-tagged *AvrLm1* and HA-tagged *BnMPK9* were co-expressed in *N. benthamiana*. Proteins were extracted after 48 hr and subjected to immunoprecipitation by HA-magnetic beads. Immunoprecipitated proteins (IPs) were analyzed by immunoblotting and probing with either anti-HA (α-HA) or anti-GFP (α-GFP). Scale bars represent 20 μm.

AvrLm1 Enhances BnMPK9-Dependent Cell Death

Transient expression in tobacco leaves has been extensively used to rapidly establish gene function. For instance, transient expression of tomato *LeMKK4 and MAPKKKα*, *N. benthamiana MKK1*, and *B. napus MAPKKK4*, *MAPKKK18*, and *MAPKKK19* in tobacco leaves causes HR-like cell death (del Pozo et al., 2004; Li et al., 2015; Pedley and Martin, 2004; Sun et al., 2014; Takahashi et al., 2007). *BnMPK9* was transiently expressed in *N. benthamiana* leaves via agroinfiltration. HR-like cell death developed extensively by 5 days after *BnMPK9* infiltration, whereas no HR was observed with the control *BnMPK3* (Figure 6A). To examine whether BnMPK9-dependent cell death is regulated by its phosphorylation activity, a mutated version of *BnMPK9* was generated, in which the predicted TDY phosphorylation sites were mutated (BnMPK9-mTDY). As shown in Figure 6A, BnMPK9-mTDY failed to induce cell death when infiltrated in tobacco leaves, indicating that phosphorylation activity is required for the BnMPK9-induced cell death.

Since AvrLm1 physically interacts with BnMPK9 *in vivo*, we examined whether AvrLm1 can influence BnMPK9-induced cell death. For this *BnMPK9* was co-expressed with *ΔspAvrLm1* (AvrLm1 without its native signal peptide). GFP was used as a negative control. Interestingly, co-expression of *ΔspAvrLm1* and *BnMPK9* enhanced the development of BnMPK9-induced cell death in the infiltrated region (Figure 6B), resulting in earlier development of visible cell death phenotype (as early as 3 days post-infiltration) compared with control *BnMPK9* co-infiltrated with *GFP*, which showed cell death at 4 days post-infiltration.

AvrLm1 Stabilizes Accumulation and Enhances BnMPK9 Phosphorylation

Based on the presented evidences that AvrLm1 interacts with BnMPK9 and enhances BnMPK9-induced cell death, we investigated the stability and level of accumulation of BnMPK9 in the presence of AvrLm1

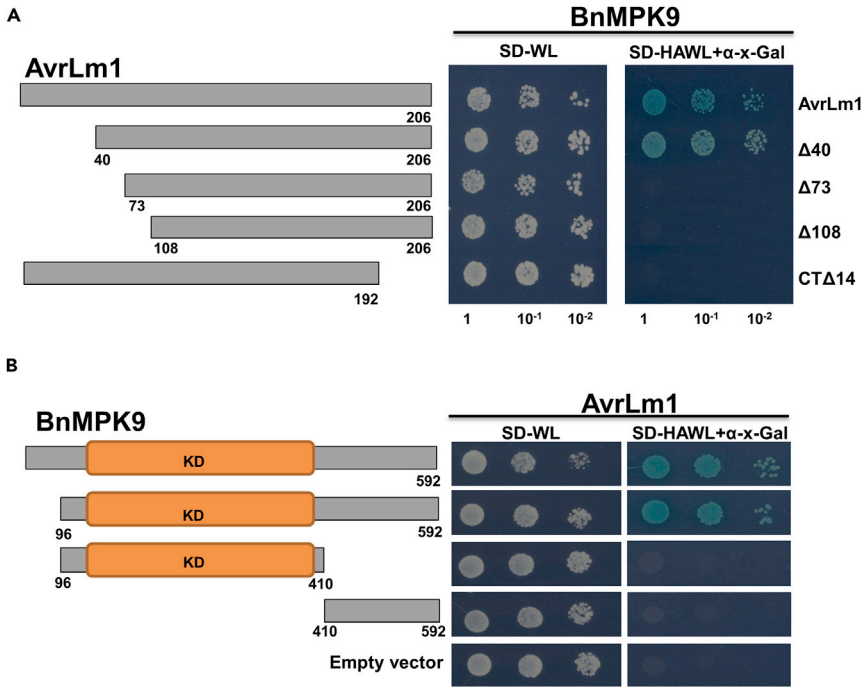

Figure 5. N-Terminal Region of AvrLm1 Is Dispensable for the Interaction with BnMPK9

(A) Truncated AvrLm1 constructs were generated including N-terminal deletion of residues 1 to 40 (Δ40), deletion of residues 40 to 73 (Δ73), deletion of residues of 70–108 (Δ108), and C-terminal deletion of residues 192–206 (CTΔ14). Each of the constructs was co-transformed with *BnMPK9* into yeast. All transformants are able to grow on synthetic dropout medium without leucine and tryptophan (SD-WL) medium. Yeast colonies that were able to grow on selective medium (SD medium without leucine, tryptophan, histidine, and adenine supplemented with X-α-Gal and Aureobasidin A [SD-HAWL]) and displayed blue coloration confirmed the protein-protein interaction.

(B) Three truncations of BnMPK9 were generated that included a small N-terminal deletion (95 aa), kinase domain of BnMPK9, and the remaining segment. Only *BnMPK9* carrying a small N-terminal deletion enabled the growth of yeast on selective plate, while no interactions were detected between AvrLm1 and any of the other two truncated constructs.

protein. HA and StrepII tags were added to *BnMPK9* and *ΔspAvrLm1,* respectively. *BnMPK9-HA* was co-expressed in *N. benthamiana* with *ΔspAvrLm1-StrepII* or *GFP* (negative control) using agroinfiltration. As shown in Figure S8, BnMPK9-HA accumulated to a higher level in the presence of ΔspAvrLm1-StrepII compared with the GFP control. The ubiquitin/26S proteasome pathway is the major proteolysis machinery in eukaryotic cells, removing most abnormal peptides and short-lived cellular regulators (Sadanandom et al., 2012). We examined and compared the stability and accumulation of BnMPK9 in the presence or absence of MG132, a proteasome inhibitor. *N. benthamiana* leaves co-expressing *BnMPK9-HA* and Δsp*AvrLm1-StrepII* or *GFP* were pre-treated with proteasomal inhibitor MG132. MG132 application resulted in increased accumulation of BnMPK9 in the leaves of control treatment (co-expressing *BnMPK9-HA* and *GFP*), to a similar level of accumulation of BnMPK9 that was observed in the leaves co-expressing *BnMPK9-HA* and Δsp*AvrLm1-StrepII* (Figure 7A). However, to ensure that overexpression of *AvrLm1* does not interfere with the *MPK9* expression level, we measured the *AtMPK9* expression in wild-type Col and Col-AvrLm1 transgenic lines. *AtMPK9* expression profile in Col plants overexpressing AvrLm1 was similar to the Col wild-type (Figure S9), proving that the effect of AvrLm1 on MPk9 is only at the protein level. Taken together, these observations suggest that AvrLm1 stabilizes BnMPK9 by preventing its degradation via the ubiquitin/26S proteasome pathway.

It has been demonstrated that the TDY phosphorylation site of BnMPK9 is essential for its cell death function. Thus, we hypothesized that AvrLm1 might affect the phosphorylation of BnMPK9. HA-tagged *BnMPK9* was co-expressed with *ΔspAvrLm1-StrepII* in *N. benthamiana* leaves. *BnMPK9* and *GFP* co-expression served as a negative control. HA-magnetic beads were used to immunoprecipitate transiently expressed *BnMPK9* from the *N. benthamiana* leaves in the presence of MG132. The level of phosphorylation of BnMPK9 was determined by immunoblot using anti-phosphothreonine monoclonal antibodies. As shown in Figure 7B, the *AvrLm1*

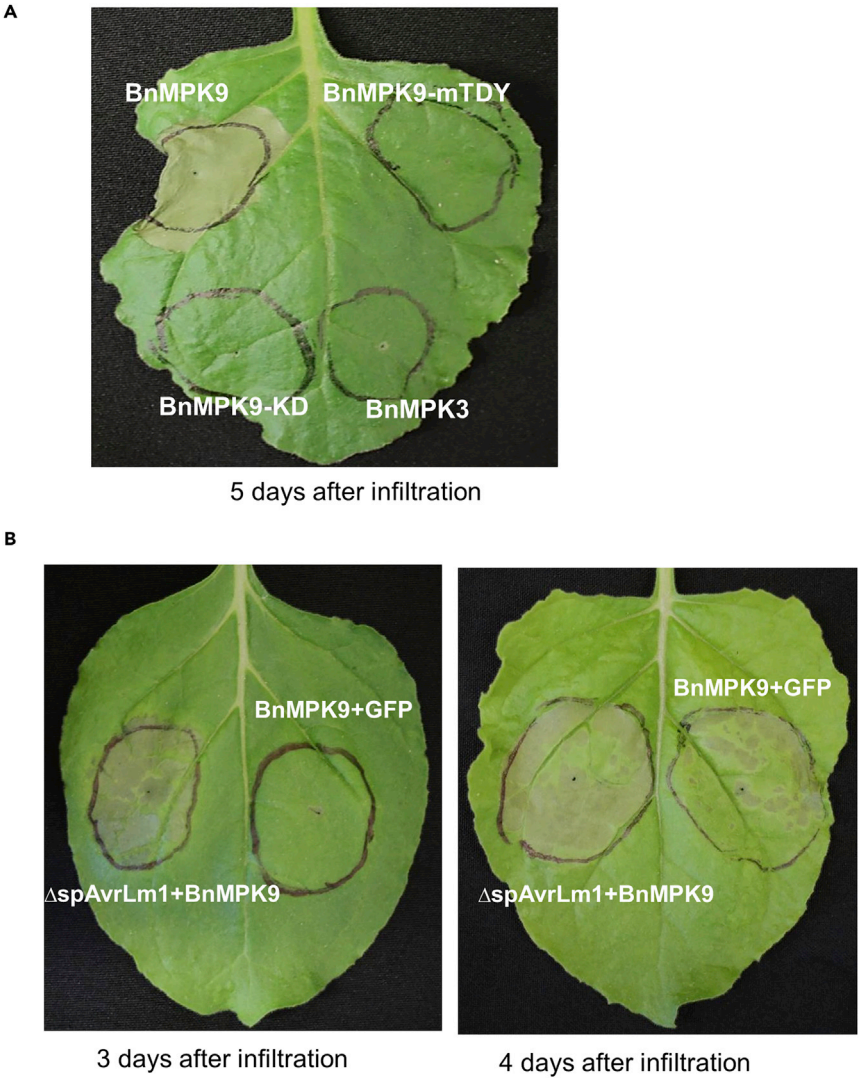

Figure 6. AvrLm1 Enhances the Development of BnMPK9-Dependent Cell Death

(A) BnMPK9 triggers cell death, and the plant-specific TDY phosphorylation motif is required for the induction of cell death. *N. benthamiana* leaves were infiltrated with *Agrobacterium* carrying *BnMPK9* or truncated *BnMPK9* encoding the kinase domain (*BnMPK9-KD*) or mutated TDY motif (*BnMPK9-mTDY*). BnMPK3 was included as a control. Representative pictures were taken 5 days post-infiltration.

(B) Co-expression of *AvrLm1* and *BnMPK9* enhanced the development of BnMPK9-induced cell death. *N. benthamiana* leaves co-infiltrated with *Agrobacterium* strains carrying *AvrLm1* and *BnMPK9* or *GFP*. The representative pictures were taken 3 and 4 days post-infiltration.

transgene specifically enhanced the phosphorylation of BnMPK9. BnMPK9 purified from *N. benthamiana* leaves infiltrated with *BnMPK9* and *GFP* showed a basal level of phosphorylation (Figure 7B), which could be due to MPK9 autophosphorylation as recently reported by Nagy et al. (Nagy et al., 2015).

Overexpression of *BnMPK9* Enhances Production of Hydrogen Peroxide in *Brassica napus*

Since AvrLm1 stabilizes BnMPK9 accumulation and enhances its phosphorylation, we examined the effect of *BnMPK9* in response to *L. maculans* infection. We initially performed RNA interference (RNAi) silencing to knockdown the expression of *BnMPK9* in Topas DH16516. Despite several attempts, we failed to generate the transgenic *B. napus* plant carrying the *BnMPK9* RNAi construct. Failure to generate MPK9 knockouts in *Arabidopsis* has also been reported (Jammes et al., 2009). However, we were successful in generating *BnMPK9* overexpression *B. napus* lines. Three homozygous single-insert *B. napus* Topas

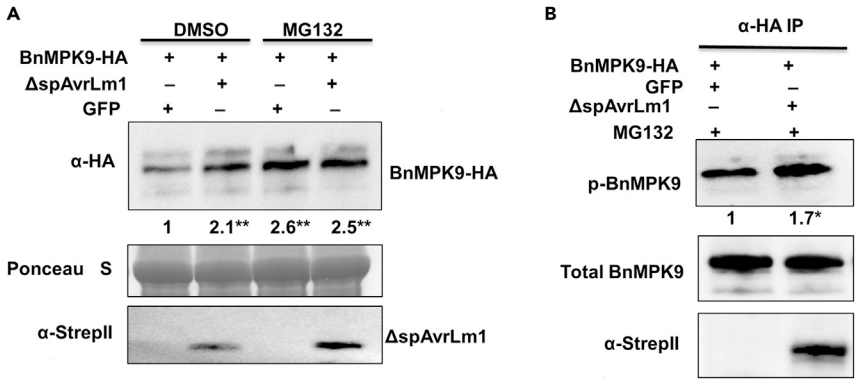

Figure 7. AvrLm1 Stabilizes the Accumulation of BnMPK9 and Enhances the Phosphorylation of BnMPK9 *in planta*

(A) Western blots probed with anti-HA and anti-StrepII antibodies showing the stabilization of BnMPK9 in the presence of AvrLm1 or 26S proteasome inhibitor (MG132). HA-tagged *BnMPK9* was co-expressed with StrepII-tagged *AvrLm1* or *GFP* in *N. benthamiana* leaves using agroinfiltration. Dimethyl sulfoxide (DMSO) or MG132 (100 mM) was infiltrated into the leaves at 24 hr post-infiltration. Proteins were extracted after 48 hr post-infiltration and subjected to western blotting. Numbers below the blots represent relative abundances of BnMPK9. ImageJ was employed to quantify the protein bands. ** represents the significant differences ($p < 0.01$, one-way analysis of variance [ANOVA]). Ponceau S (PS) staining shows equal amount of protein loaded in each well.

(B) Western blot probed with anti-HA and anti-phosphothreonine monoclonal antibody showing the enhanced phosphorylation of BnMPK9 in the presence of Avrlm1. HA-tagged *BnMPK9* was co-expressed with StrepII-tagged *AvrLm1* or *GFP* in *N. benthamiana* leaves using agroinfiltration, and MG132 (100 mM) was infiltrated into the leaves at 24 hr post-infiltration. Proteins were extracted 48 hr post-infiltration and immunoprecipitated with HA magnetic beads. Numbers below the blots represent relative abundances of phosphorylated BnMPK9, and quantification of phosphorylated BnMPK9 was performed using ImageJ by normalizing to total amount of BnMPK9 protein. * represents the significant differences ($p < 0.05$, one-way ANOVA). Total BnMP9 protein loading is shown with anti-HA antibody. The experiments were repeated three times with consistent results.

DH16516 lines in which the *BnMPK9* expression was driven by the 35S promoter were generated. Overexpression of *BnMPK9* (15–20 fold) in these lines was confirmed by qRT-PCR (Figure S10). As described above, transient expression of *BnMPK9* induces cell death in *N. benthamiana* plants (Figure 6); however, transgenic *B. napus* lines overexpressing *BnMPK9* grew normally and did not display any visual cell death symptoms. High accumulation of hydrogen peroxide has been used as an indicator of cell death. To detect the H_2O_2 production, *BnMPK9*-overexpressing lines were stained by 3,3-Diaminobenzidine (DAB). Interestingly, we observed pronounced staining for hydrogen peroxide in the cotyledons of *BnMPK9*-overexpressing lines. By contrast, the cotyledon of control line Topas DH16516 showed only weak staining (Figure 8). To further confirm this observation, we measured the production of hydrogen peroxide in cotyledons infected with *L. maculans* isolate v23.1.3. The intensively stained area, due to H_2O_2 production, was much larger in cotyledons overexpressing *BnMPK9* than in control plant (Figure 8). Taken together, it could be concluded that overexpression of *BnMPK9* enhances the production of hydrogen peroxide, while no cotyledon of transgenic lines shows any macroscopically visible cell deaths.

Overexpression of BnMPK9 Enhances *L. maculans* Growth in *Brassica napus*

Expression of SA marker genes *PR1* and *WRKY70*, and JA-related genes *LOX3* and *AOS*, was measured by qRT-PCR in Topas DH16516 overexpressing *BnMPK9* and the control Topas DH16516 lines. *PR1* and *WRKY70* expression levels were reduced to 70% and 30% compared with the control, respectively. In contrast, the expression levels of *LOX3* and *AOS* were slightly elevated in the *BnMPK9* overexpression lines (Figure 9). Two *BnMPK9* transgenic lines were inoculated with the *L. maculans* isolate v23.1.3. Topas DH16516 that is susceptible to *L. maculans* was included as a positive control. At 8 dpi enhanced disease development was evident as formation of larger lesion on the cotyledons of Topas:*BnMPK9* compared with the control (Figures 10A and 10B). Next, disease development was monitored over time. Asexual spore (pycnidiospore) formation, seen as black dots formed within the lesion, was more prevalent in the *BnMPK9* overexpression lines at 10, 12, and 14 dpi (Figure 10A). Furthermore, the amount of fungal DNA in the cotyledons of *BnMPK9*-overexpresing and wild-type Topas lines was quantified by quantitative PCR (qPCR) analysis of *L. maculans*' *LmITS1* DNA at 8 dpi. Higher levels of *L. maculans* DNA in the

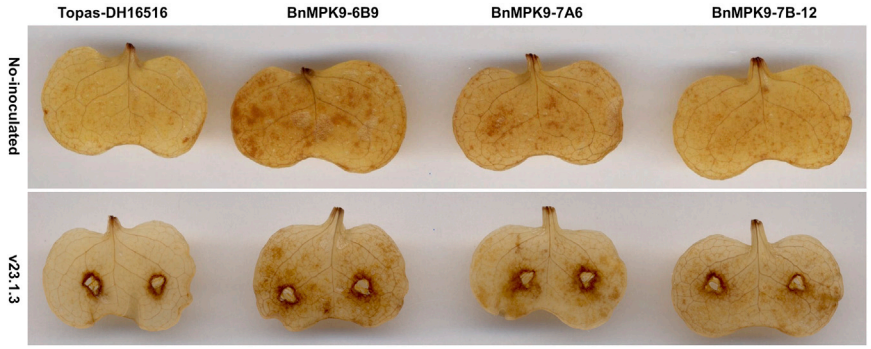

Figure 8. DAB Staining of Hydrogen Peroxide in *BnMPK9*-Overexpresing *B. napus* Lines

Cotyledons of 7-day-old Topas DH16516 seedlings and three *BnMPK9*-overexpressing *B. napus* lines were inoculated on wound sites using a spore suspension of *L. maculans* isolate v23.1.3. Four day post-inoculation, detached non-inoculated and inoculated cotyledons were used for DAB staining.

Topas:*BnMPK9* provided additional support that overexpression of *BnMPK9* enhances the susceptibility of *B. napus* to *L. maculans* (Figure 10C).

DISCUSSION

B. napus resistance at the seedling stage to *L. maculans* is conferred by race-specific resistance genes. Despite significant advances in defining the genetics of the *B. napus*-*L. maculans* interaction, including isolation of two *R* genes and several *Avr* genes (Raman et al., 2013), up to now information about the molecular interaction and function of R/Avr proteins for the *B. napus*-*L. maculans* pathosystem has been lacking. The study presented here is the first report that describes the virulence function of an *L. maculans* effector by identifying its target in *B. napus*. We identified BnMPK9 as the host target of AvrLm1 and determined their interaction both *in vitro* and *in planta*. The BnMPK9-AvrLm1 interaction enhances cell death caused by BnMPK9, and mutation within kinase domain of BnMPK9 abolishes cell death. We further showed that AvrLm1 stabilizes the accumulation and facilitates the phosphorylation of BnMPK9, leading to the development of enhanced cell death in tobacco. Furthermore, overexpression of *BnMPK9* perturbs hormone signaling pathways and enhances the growth of *L. maculans* in *B. napus*. Together, these results uncover a novel role for *BnMPK9* in plant defense and its modulation by a fungal effector, causing enhanced plant susceptibility.

L. maculans is an intercellular pathogen, and not surprisingly, the LepR3 protein, the *B. napus* receptor for AvrLm1, is a membrane-bound RLP. To gain insight into the localization of AvrLm1, we tracked the AvrLm1-mCherry fusion protein expressed in *L. maculans* during infection of *B. napus* cotyledon tissues. Although we could not detect mCherry fluorescent signals inside the host plant cells, we frequently observed accumulation of mCherry signals at the focal points of contact between the fungal hyphae and plant host mesophyll cells. In addition, proof of function of AvrLm1 signal peptide in yeast (Figure S11) and enrichment of AvrLm1 protein in the apoplastic fluid of *B. napus* tissue infected with *L. maculans* (Figure S3) provided further evidence that *L. maculans* secretes AvrLm1 into the host apoplast. *AvrLm1* encodes a protein with one cysteine residue, which is atypical for the commonly reported apoplastic fungal effector proteins (Fudal et al., 2007), indicating that AvrLm1 may enter into plant cell to avoid the harsh environment of the apoplast. Therefore, lack of discernible red fluorescent signals inside the host cell may be due to the rapid diffusion of AvrLm1-mCherry protein, reducing fluorescent signals to a level below our detection limits. Similar technical limitations have been reported for the translocation studies of fluorescently labeled effectors from other filamentous pathogens sash as the RXLR effectors from oomycetes or effectors from *Colletotrichum higginsianum* (Jing et al., 2016; Kleemann et al., 2012). Alternative localization techniques reported recently, such as the split fluorescent GFP system, may overcome these technical limitations (Henry et al., 2017; Park et al., 2017).

The physical interaction between AvrLm1 and BnMPK9 results in increased accumulation and enhanced phosphorylation of BnMPK9 (Figure 7). So far, there has been no report of a fungal effector directly targeting the MAPK pathway. The only example from filamentous pathogens is the *P. infestans* RXLR effector PexRD2, which has been reported to interact with host MAPKKKε and suppress MAPKKKε-dependent cell death to perturb plant immune signaling (King et al., 2014). However, accumulating evidences from

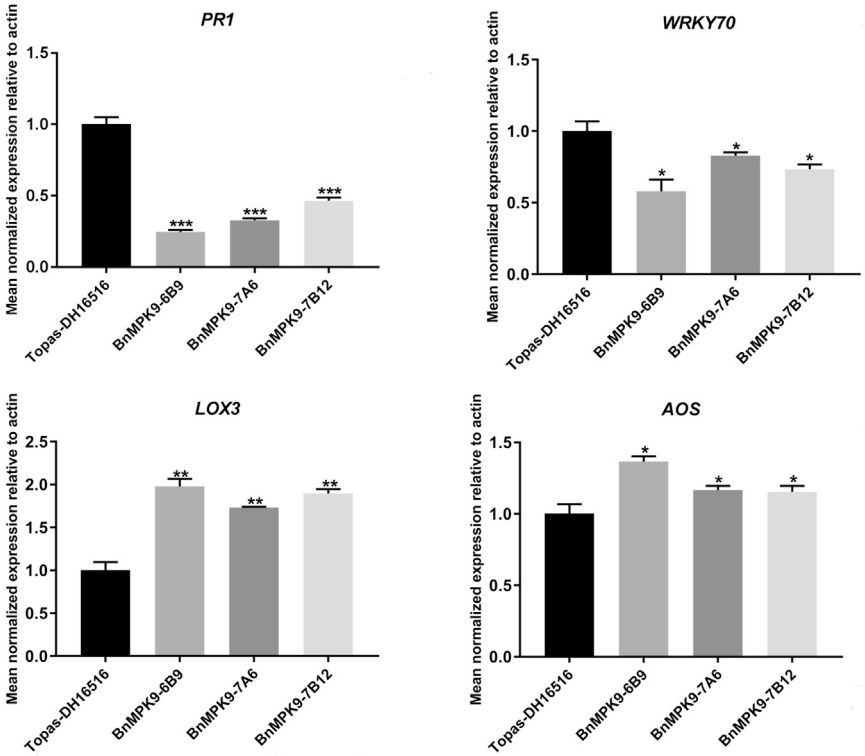

Figure 9. Relative Expression of Salicylic Acid (SA) and Jasmonic Acid (JA) Marker Genes in *BnMPK9*-Overexpressing *B. napus* Lines

Cotyledons of 7-day-old seedlings of *BnMPK9*-overexpressing *B. napus* plants were collected and used for RNA extraction. Expressions of *B. napus* signaling marker genes including *PR1*, *WRKY70*, *LOX3*, and *AOS* were determined by quantitative reverse-transcriptase polymerase chain reaction and normalized to *B. napus actin*. Values represent means ± standard error (SE) from three independent experiments. *, **, and *** represent the significant differences ($p < 0.05$, $p < 0.01$, and $p < 0.001$, respectively; one-way analysis of variance [ANOVA] followed by the Turkey post-test).

studies on a variety of bacterial pathogens support that manipulation of components of MAPK kinase signaling cascade is an important virulence strategy of bacterial pathogens (Bigeard et al., 2015; Feng and Zhou, 2012). Two known MAPK modules, MKK4/MKK5-MPK3/MPK6 and MEKK1-MKK1/MKK2-MPK4 involved in plant defense signaling, are targeted by different bacterial effectors either to inactivate or enhance their kinase activities. For example, HopAI1 inactivates AtMPK3, AtMPK4, and AtMPK6 by irreversibly removing the phosphate group from the threonine residue of the MAPK activation loop (Zhang et al., 2007). *P. syringae* effector HopF2 targets AtMKK5, and the *P. syringae* effector AvrB interacts with AtMPK4 and induces the phosphorylation and activation of MPK4 (Cui et al., 2010; Wang et al., 2010). Our results provide the first example that a fungal pathogen also targets MAPK modules to manipulate plant defense response. The RLK proteins, SOBIR1 and BAK1, are components of the LepR3 receptor complex and are required for the recognition of AvrLm1 (Ma and Borhan, 2015), indicating the importance of MAPK signaling cascade downstream of the LepR3 receptor complex.

Previous studies showed that AtMPK9, together with AtMPK12, functions in ABA- and methyl jasmonate-induced stomatal closure in *Arabidopsis* (Lee et al., 2016; Jammes et al., 2009; Khokon et al., 2015) and that they act redundantly. However, our data show that AvrLm1 does not interact with MPK12, proving the specificity of AvrLm1-MPK9 interaction (Figure S7) and indicating that in the Brassicaceae, MPK12 is dispensable for the virulence function of AvrLm1. Furthermore, transient overexpression of *BnMPK9* in *N. benthamiana* resulted in cell death. However, we did not detect any visible cell death phenotype when *BnMPK12* was overexpressed in tobacco (Figure 6). These observations indicated that MPK9's function in inducing cell death and mediating *L. maculans* virulence in *B. napus* is independent of MPK12. The importance of MPKs in regulating plant immune response is well documented (Pitzschke et al., 2009; Popescu et al., 2009). Overexpression of the *N. benthamiana* homologs of AtMPK3 and AtMPK6 and *Arabidopsis*

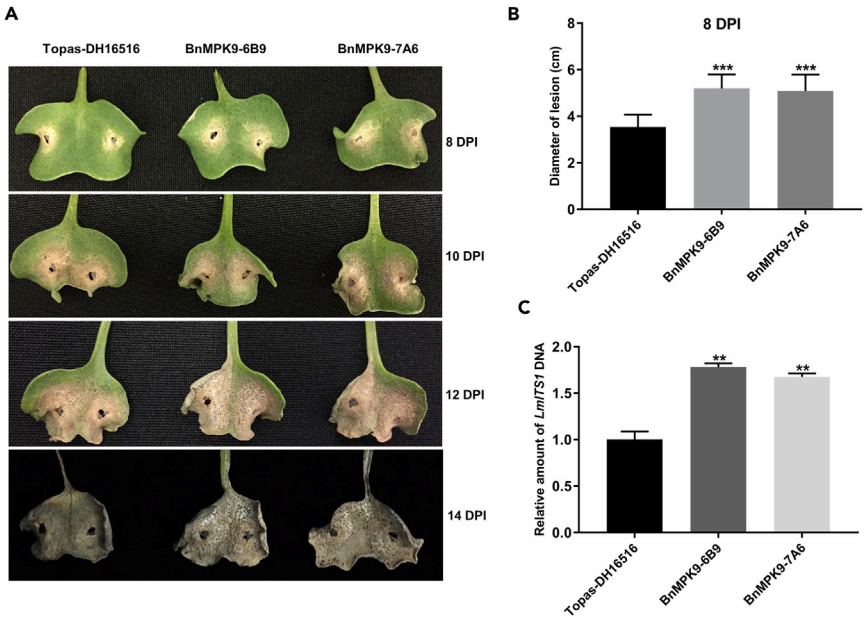

Figure 10. Expression of *BnMPK9* Results in Increased Susceptibility to *L. maculans*

Cotyledons of 7-day-old Topas DH16516 seedlings and two *BnMPK9*-expressing lines (BnMPk9-6B9 and BnMPK9-7A6) were inoculated on wound sites using a spore suspension of *L. maculans* isolate v23.1.3.

(A) Representative cotyledons at 8, 10, 12, and 14 dpi were photographed.

(B) The size of the lesions was measured at 8 dpi and statistically analyzed. Values represent means ± standard error (SE) ($n > 30$). Asterisks indicate statistically significant differences (***, $p < 0.001$, one-way analysis of variance [ANOVA]). Three independent biological experiments were conducted.

(C) qRT-PCR analysis showing the fungal mass in *L. maculans*-infected cotyledons of *B. napus* at 8 dpi. Constitutively expressed *LmITS1* gene was used as a marker showing DNA level and pathogen mass. *LmITS1 gene* expression levels were normalized to expression of *B. napus actin*. Values are means ± SE of triplicate reactions of three independent biological samples. Significant differences are represented by ** (**, $p < 0.01$, one-way ANOVA).

MKK4, MKK5, MKK7, and MKK9 cause cell death in tobacco (Popescu et al., 2009; Ren et al., 2006; Yang et al., 2001). Also, overexpression of *B. napus* MAPKKK4 causes up-regulation of genes related to reactive oxygen species accumulation, cell death, and defense response (Li et al., 2015). Plant cell death is an effective mechanism of containing the growth of biotrophic pathogens, whereas induction of cell death is a virulence mechanism employed by hemibiotrophic and necrotrophic fungi to more readily absorb nutrients from the host plant (Ding et al., 2011; Greenberg and Yao, 2004). Interestingly, previous study of the *B. napus* transcriptome in response to *L. maculans* infection revealed that the peak expression of *AvrLm1* and *NLP* (necrosis- and ethylene-inducing protein) coincide with the transition from biotrophy to necrotrophy of *L. maculans* during *B. napus* cotyledon infection (Haddadi et al., 2016). Taken together, heightened expression of *AvrLm1* by *L. maculans* leading to enhanced induction of cell death through the interaction of AvrLm1 with BnMPK9 could be perceived as a virulence mechanism supporting the transition from biotrophy to necrotrophy to facilitate the acquisition of host nutrients by *L. maculans*.

Our results show that in the *BnMPK9* transgenic *B. napus* plants, transcription of *PR-1* and *WYKR70* is significantly reduced but expression levels of *LOX3* and *AOS* are elevated, indicating suppression of the SA-dependent pathway and activation of the JA-dependent pathway. However, expression of *LOX2* gene in *AvrLm1*-overexpressing *Arabidopsis* is down-regulated. This apparent discrepancy in *LOX* gene expression could be attributed to the suggested presence of a cytoplasm- and a chloroplast-localized pathway for JA biosynthesis. LOX2 is reported to be targeted to the chloroplast (He et al., 2002). Although LOX3 is possibly targeted to the chloroplast, its expression pattern is not necessarily similar to that of *LOX2*. For instance, it was reported that *LOX3* was up-regulated during the leaf senescence, but expression of *LOX2* was significantly down-regulated (He et al., 2002). Importance of SA and JA pathways during the *L. maculans-B. napus* interaction has also been previously reported (Becker et al., 2017; Haddadi et al., 2016). In *B. napus* cotyledon tissues infected with *L. maculans*, SA-related genes were induced at the initial

phases of infection (2–4 dpi), but as the infection progressed and at the initiation of necrotrophic stage, genes related to the JA pathway were up-regulated (Haddadi et al., 2016). Thus, we hypothesize that AvrLm1 as a virulence factor facilitates the phosphorylation of BnMPK9, leading to the suppression of SA-dependent pathway and supporting the colonization of *L. maculans* at the initial infection stage. AvrLm4-7, another *L. maculans* effector, was recently reported to act as a virulence factor by suppressing the host SA signaling pathway (Nováková et al., 2016). AvrLm1 and AvrLm4-7 also contribute to the aggressiveness of *L. maculans* during leaf infection (Huang et al., 2006, 2009).

To the best of our knowledge, this is the first study to show that an effector from a fungal plant pathogen targets the MPK pathway to suppress plant host defense. Our results show that AvrLm1 supports the *L. maculans* infection by stabilizing the accumulation and inducing the phosphorylation of BnMPK9. Owing to technical limitations for genetic manipulation and also the complexity of the *B. napus* genome, most of the experiments that were carried out in the present study had to be done using the model plants *A. thaliana* and *N. benthamiana*. These model plants have been extensively used in plant biology research and proved to be invaluable in the translation of such research to crop species. However, further experiments in *B. napus* will provide additional support for the role of AvrLm1 and its target BnMPK9 in defense against *L. maculans* in its the natural host plant.

Until recently the molecular interaction of *B. napus* with the economically important blackleg pathogen *L. maculans* remained largely unknown. The research presented here expands our knowledge of the *Brassica-Leptosphaeria* pathosystem and highlights the importance of the MPK pathway, adding to our recent advances in understanding the perception of *L. maculans* and induction of downstream signaling in *B. napus*.

METHODS

All methods can be found in the accompanying Transparent Methods supplemental file.

SUPPLEMENTAL INFORMATION

Supplemental Information includes Transparent Methods, 11 figures, and 2 tables and can be found with this article online at https://doi.org/10.1016/j.isci.2018.04.015.

ACKNOWLEDGMENTS

We thank Helen Lui for generating the *L. maculans*-YFP transgenic line. Funding for this research was provided by AAFC, SaskCanola and Alberta Canola Producers Commission (Grant number: AIP-P032).

AUTHOR CONTRIBUTIONS

L.M. and M.H.B. designed the experiments and prepared the manuscript. L.M. conducted the majority of the experiments. M. D., H.W., N.J.L., P.H., E.B., and G.G. contributed to the experiments and read the manuscript. N.J.L. edited the manuscript.

DECLARATION OF INTERESTS

The authors declare no conflict of interest.

Received: November 9, 2017
Revised: March 22, 2018
Accepted: April 16, 2018
Published: May 25, 2018

REFERENCES

Asai, T., Tena, G., Plotnikova, J., Willmann, M.R., Chiu, W.-L., Gomez-Gomez, L., Boller, T., Ausubel, F.M., and Sheen, J. (2002). MAP kinase signalling cascade in *Arabidopsis* innate immunity. Nature *415*, 977–983.

Becker, M.G., Zhang, X., Walker, P.L., Wan, J.C., Millar, J.L., Khan, D., Granger, M.J., Cavers, J.D., Chan, A.C., Fernando, D.W.G., et al. (2017). Transcriptome analysis of the *Brassica napus–Leptosphaeria maculans* pathosystem identifies receptor, signaling and structural genes underlying plant resistance. Plant J. *90*, 573–586.

Bigeard, J., Colcombet, J., and Hirt, H. (2015). Signaling mechanisms in pattern-triggered immunity (PTI). Mol. Plant *8*, 521–539.

Block, A., and Alfano, J.R. (2011). Plant targets for *Pseudomonas syringae* type III effectors: virulence targets or guarded decoys? Curr. Opin. Microbiol. *14*, 39–46.

Chalhoub, B., Denoeud, F., Liu, S., Parkin, I.A.P., Tang, H., Wang, X., Chiquet, J., Belcram, H., Tong, C., Samans, B., et al. (2014). Early allopolyploid evolution in the post-Neolithic

Brassica napus oilseed genome. Science *345*, 950–953.

Cui, H., Wang, Y., Xue, L., Chu, J., Yan, C., Fu, J., Chen, M., Innes, R.W., and Zhou, J.-M. (2010). *Pseudomonas syringae* effector protein AvrB perturbs Arabidopsis hormone signaling by activating MAP kinase 4. Cell Host Microbe *7*, 164–175.

de Jonge, R., Peter van Esse, H., Kombrink, A., Shinya, T., Desaki, Y., Bours, R., van der Krol, S., Shibuya, N., Joosten, M.H.A.J., and Thomma, B.P.H.J. (2010). Conserved fungal LysM effector Ecp6 prevents chitin-triggered immunity in plants. Science *329*, 953–955.

del Pozo, O., Pedley, K.F., and Martin, G.B. (2004). MAPKKKα is a positive regulator of cell death associated with both plant immunity and disease. EMBO J. *23*, 3072–3082.

Deslandes, L., and Rivas, S. (2012). Catch me if you can: bacterial effectors and plant targets. Trends Plant Sci. *17*, 644–655.

Ding, L., Xu, H., Yi, H., Yang, L., Kong, Z., Zhang, L., Xue, S., Jia, H., and Ma, Z. (2011). Resistance to hemi-biotrophic *F. graminearum* infection is associated with coordinated and ordered expression of diverse defense signaling pathways. PLoS One *6*, e19008.

Felix, G., Duran, J.D., Volko, S., and Boller, T. (1999). Plants have a sensitive perception system for the most conserved domain of bacterial flagellin. Plant J. *18*, 265–276.

Feng, F., and Zhou, J.-M. (2012). Plant–bacterial pathogen interactions mediated by type III effectors. Curr. Opin. Plant Biol. *15*, 469–476.

Fisher, M.C., Henk, D.A., Briggs, C.J., Brownstein, J.S., Madoff, L.C., McCraw, S.L., and Gurr, S.J. (2012). Emerging fungal threats to animal, plant and ecosystem health. Nature *484*, 186–194.

Fudal, I., Ross, S., Gout, L., Blaise, F., Kuhn, M.L., Eckert, M.R., Cattolico, L., Bernard-Samain, S., Balesdent, M.H., and Rouxel, T. (2007). Heterochromatin-like regions as ecological niches for Avirulence genes in the *Leptosphaeria maculans* genome: map-based cloning of AvrLm6. Mol. Plant Microbe Interact. *20*, 459–470.

Gao, M., Liu, J., Bi, D., Zhang, Z., Cheng, F., Chen, S., and Zhang, Y. (2008). MEKK1, MKK1/MKK2 and MPK4 function together in a mitogen-activated protein kinase cascade to regulate innate immunity in plants. Cell Res. *18*, 1190–1198.

Gout, L., Fudal, I., Kuhn, M.-L., Blaise, F., Eckert, M., Cattolico, L., Balesdent, M.-H., and Rouxel, T. (2006). Lost in the middle of nowhere: the AvrLm1 avirulence gene of the dothideomycete *Leptosphaeria maculans*. Mol. Microbiol. *60*, 67–80.

Greenberg, J.T., and Yao, N. (2004). The role and regulation of programmed cell death in plant–pathogen interactions. Cell. Microbiol. *6*, 201–211.

Haddadi, P., Ma, L., Wang, H., and Borhan, M.H. (2016). Genome-wide transcriptomic analyses provide insights into the lifestyle transition and effector repertoire of *Leptosphaeria maculans* during the colonization of Brassica napus seedlings. Mol. Plant Pathol. *8*, 1196–1210.

Henry, E., Toruño, T.Y., Jauneau, A., Deslandes, L., and Coaker, G.L. (2017). Direct and indirect visualization of bacterial effector delivery into diverse plant cell types during infection. Plant Cell *29*, 1555–1570.

He, Y., Fukushige, H., Hildebrand, D.F., and Gan, S. (2002). Evidence supporting a role of jasmonic acid in *Arabidopsis* leaf senescence. Plant Physiol. *128*, 876–884.

Huang, Y.-J., Balesdent, M.-H., Li, Z.-Q., Evans, N., Rouxel, T., and Fitt, B.D.L. (2009). Fitness cost of virulence differs between the AvrLm1 and AvrLm4 loci in *Leptosphaeria maculans* (phoma stem canker of oilseed rape). Eur. J. Plant Pathol. *126*, 279.

Huang, Y.-J., Li, Z.-Q., Evans, N., Rouxel, T., Fitt, B.D.L., and Balesdent, M.-H. (2006). Fitness cost associated with loss of the AvrLm4 avirulence function in *Leptosphaeria maculans* (phoma stem canker of oilseed rape). Eur. J. Plant Pathol. *114*, 77–89.

Ichimura, K., Shinozaki, K., Tena, G., Sheen, J., Henry, Y., Champion, A., Kreis, M., Zhang, S., Hirt, H., et al. (2002). Mitogen-activated protein kinase cascades in plants: a new nomenclature. Trends Plant Sci. *7*, 301–308.

Jammes, F., Song, C., Shin, D., Munemasa, S., Takeda, K., Gu, D., Cho, D., Lee, S., Giordo, R., Sritubtim, S., et al. (2009). MAP kinases MPK9 and MPK12 are preferentially expressed in guard cells and positively regulate ROS-mediated ABA signaling. Proc. Natl. Acad. Sci. USA *106*, 20520–20525.

Jammes, F., Yang, X., Xiao, S., and Kwak, J.M. (2011). Two *Arabidopsis* guard cell-preferential MAPK genes, MPK9 and MPK12, function in biotic stress response. Plant Signal. Behav. *6*, 1875–1877.

Jing, M., Guo, B., Li, H., Yang, B., Wang, H., Kong, G., Zhao, Y., Xu, H., Wang, Y., Ye, W., et al. (2016). A *Phytophthora sojae* effector suppresses endoplasmic reticulum stress-mediated immunity by stabilizing plant binding immunoglobulin proteins. Nat. Commun. *7*, 11685.

Jones, J.D.G., and Dangl, J.L. (2006). The plant immune system. Nature *444*, 323–329.

Khokon, M.A.R., Salam, M.A., Jammes, F., Ye, W., Hossain, M.A., Okuma, E., Nakamura, Y., Mori, I.C., Kwak, J.M., and Murata, Y. (2017). MPK9 and MPK12 function in SA-induced stomatal closure in *Arabidopsis thaliana*. Biosci. Biotechnol. Biochem. *81*, 1394–1400.

Khokon, M.A.R., Salam, M.A., Jammes, F., Ye, W., Hossain, M.A., Uraji, M., Nakamura, Y., Mori, I.C., Kwak, J.M., and Murata, Y. (2015). Two guard cell mitogen-activated protein kinases, MPK9 and MPK12, function in methyl jasmonate-induced stomatal closure in *Arabidopsis thaliana*. Plant Biol. (Stuttg.) *17*, 946–952.

King, S.R.F., McLellan, H., Boevink, P.C., Armstrong, M.R., Bukharova, T., Sukarta, O., Win, J., Kamoun, S., Birch, P.R.J., and Banfield, M.J. (2014). *Phytophthora infestans* RXLR effector PexRD2 interacts with host MAPKKKε to suppress plant immune signaling. Plant Cell *26*, 1345–1359.

Kleemann, J., Rincon-Rivera, L.J., Takahara, H., Neumann, U., Ver Loren van Themaat, E., van der Does, H.C., Hacquard, S., Stuber, K., Will, I., Schmalenbach, W., et al. (2012). Sequential delivery of host-induced virulence effectors by appressoria and intracellular hyphae of the phytopathogen *Colletotrichum higginsianum*. PLoS Pathog. *8*, e1002643.

Klevernic, I.V., Stafford, M.J., Morrice, N., Peggie, M., Morton, S., and Cohen, P. (2006). Characterization of the reversible phosphorylation and activation of ERK8. Biochem. J. *394*, 365–373.

Larkan, N.J., Lydiate, D.J., Parkin, I.A.P., Nelson, M.N., Epp, D.J., Cowling, W.A., Rimmer, S.R., and Borhan, M.H. (2013). The Brassica napus blackleg resistance gene *LepR3* encodes a receptor-like protein triggered by the *Leptosphaeria maculans* effector AVRLM1. New Phytol. *197*, 595–605.

Larkan, N.J., Ma, L., and Borhan, M.H. (2015). The *Brassica napus* receptor-like protein RLM2 is encoded by a second allele of the LepR3/Rlm2 blackleg resistance locus. Plant Biotechnol. J. *13*, 983–992.

Larkan, N.J., Yu, F., Lydiate, D.J., Rimmer, S.R., and Borhan, M.H. (2016). Single R gene introgression lines for accurate dissection of the *Brassica - Leptosphaeria* pathosystem. Front. Plant Sci. *7*, 1771.

Lee, Y., Kim, Y.J., Kim, M.-H., and Kwak, J.M. (2016). MAPK cascades in guard cell signal transduction. Front. Plant Sci. *7*, 80.

Li, L., Ye, C., Zhao, R., Li, X., Liu, W.-Z., Wu, F., Yan, J., Jiang, Y.-Q., and Yang, B. (2015). Mitogen-activated protein kinase kinase kinase (MAPKKK) 4 from rapeseed (*Brassica napus* L.) is a novel member inducing ROS accumulation and cell death. Biochem. Biophys. Res. Commun. *467*, 792–797.

Ma, L., and Borhan, H. (2015). The receptor-like kinase SOBIR1 interacts with *Brassica napus* LepR3 and is required for *Leptosphaeria maculans* AvrLm1-triggered immunity. Front. Plant Sci. *6*, 933.

Meng, X., and Zhang, S. (2013). MAPK cascades in plant disease resistance signaling. Annu. Rev. Phytopathol. *51*, 245–266.

Montillet, J.-L., Leonhardt, N., Mondy, S., Tranchimand, S., Rumeau, D., Boudsocq, M., Garcia, A.V., Douki, T., Bigeard, J., Laurière, C., et al. (2013). An abscisic acid-independent oxylipin pathway controls stomatal closure and immune defense in Arabidopsis. PLoS Biol. *11*, e1001513.

Nagy, S.K., Darula, Z., Kállai, B.M., Bögre, L., Bánhegyi, G., Medzihradszky, K.F., Horváth, G.V., and Mészáros, T. (2015). Activation of AtMPK9 through autophosphorylation that makes it independent of the canonical MAPK cascades. Biochem. J. *467*, 167–175.

Nováková, M., Šašek, V., Trdá, L., Krutinová, H., Mongin, T., Valentová, O., Balesdent, M.-H., Rouxel, T., and Burketová, L. (2016). *Leptosphaeria maculans* effector AvrLm4-7 affects salicylic acid (SA) and ethylene (ET)

signalling and hydrogen peroxide (H2O2) accumulation in *Brassica napus*. Mol. Plant Pathol. *17*, 818–831.

Park, E., Lee, H.-Y., Woo, J., Choi, D., and Dinesh-Kumar, S.P. (2017). Spatiotemporal monitoring of *Pseudomonas syringae* effectors via type III secretion using split fluorescent protein fragments. Plant Cell *29*, 1571–1584.

Pedley, K.F., and Martin, G.B. (2004). Identification of MAPKs and their possible MAPK kinase activators involved in the Pto-mediated defense response of tomato. J. Biol. Chem. *279*, 49229–49235.

Pitzschke, A., Schikora, A., and Hirt, H. (2009). MAPK cascade signalling networks in plant defence. Curr. Opin. Plant Biol. *12*, 421–426.

Popescu, S., Popescu, G., Bachan, S., Zhang, Z., Gerstein, M., Snyder, M., and Dinesh-Kumar, S. (2009). MAPK target networks in *Arabidopsis thaliana* revealed using functional protein microarrays. Genes Dev. *23*, 80–92.

Presti, L.L., Lanver, D., Schweizer, G., Tanaka, S., Liang, L., Tollot, M., Zuccaro, A., Reissmann, S., and Kahmann, R. (2015). Fungal effectors and plant susceptibility. Annu. Rev. Plant Biol. *66*, 513–545.

Raman, H., Raman, R., and Larkan, N. (2013). Genetic dissection of blackleg resistance loci in rapeseed (*Brassica napus* L. In Plant Breeding from Laboratories to Fields, S.B. Andersen, ed. (InTech), Ch. 04.

Rasmussen, M.W., Roux, M., Petersen, M., and Mundy, J. (2012). MAP kinase cascades in *Arabidopsis* innate immunity. Front. Plant Sci. *3*, 169.

Ren, D., Yang, K.-Y., Li, G.-J., Liu, Y., and Zhang, S. (2006). Activation of Ntf4, a tobacco mitogen-activated protein kinase, during plant defense response and its involvement in hypersensitive response-like cell death. Plant Physiol. *141*, 1482–1493.

Sadanandom, A., Bailey, M., Ewan, R., Lee, J., and Nelis, S. (2012). The ubiquitin–proteasome system: central modifier of plant signalling. New Phytol. *196*, 13–28.

Sánchez-Vallet, A., Saleem-Batcha, R., Kombrink, A., Hansen, G., Valkenburg, D.-J., Thomma, B.P.H.J., and Mesters, J.R. (2013). Fungal effector Ecp6 outcompetes host immune receptor for chitin binding through intrachain LysM dimerization. Elife *2*, e00790.

Stergiopoulos, I., and de Wit, P.J. (2009). Fungal effector proteins. Annu. Rev. Phytopathol. *47*, 233–263.

Sun, Y., Wang, C., Yang, B., Wu, F., Hao, X., Liang, W., Niu, F., Yan, J., Zhang, H., Wang, B., et al. (2014). Identification and functional analysis of mitogen-activated protein kinase kinase kinase (MAPKKK) genes in canola (*Brassica napus L.*). J. Exp. Bot. *65*, 2171–2188.

Takahashi, Y., Nasir, K.H.B., Ito, A., Kanzaki, H., Matsumura, H., Saitoh, H., Fujisawa, S., Kamoun, S., and Terauchi, R. (2007). A high-throughput screen of cell-death-inducing factors in *Nicotiana benthamiana* identifies a novel MAPKK that mediates INF1-induced cell death signaling and non-host resistance to *Pseudomonas cichorii*. Plant J. *49*, 1030–1040.

van den Burg, H.A., Westerink, N., Francoijs, K.-J., Roth, R., Woestenenk, E., Boeren, S., de Wit, P.J.G.M., Joosten, M.H.A.J., and Vervoort, J. (2003). Natural disulfide bond-disrupted mutants of AVR4 of the tomato pathogen *Cladosporium fulvum* are sensitive to proteolysis, circumvent Cf-4-mediated resistance, but retain their chitin binding ability. J. Biol. Chem. *278*, 27340–27346.

Wang, Y., Li, J., Hou, S., Wang, X., Li, Y., Ren, D., Chen, S., Tang, X., and Zhou, J.-M. (2010). A *Pseudomonas syringae* ADP-ribosyltransferase inhibits Arabidopsis mitogen-activated protein kinase kinases. Plant Cell *22*, 2033–2044.

West, J.S., Kharbanda, P.D., Barbetti, M.J., and Fitt, B.D.L. (2001). Epidemiology and management of *Leptosphaeria maculans* (phoma stem canker) on oilseed rape in Australia, Canada and Europe. Plant Pathol. *50*, 10–27.

Win, J., Chaparro-Garcia, A., Belhaj, K., Saunders, D.G.O., Yoshida, K., Dong, S., Schornack, S., Zipfel, C., Robatzek, S., Hogenhout, S.A., et al. (2012). Effector biology of plant-associated organisms: concepts and perspectives. Cold Spring Harb. Symp. Quant. Biol. *77*, 235–247.

Yang, K.-Y., Liu, Y., and Zhang, S. (2001). Activation of a mitogen-activated protein kinase pathway is involved in disease resistance in tobacco. Proc. Natl. Acad. Sci. USA *98*, 741–746.

Zhang, J., Shao, F., Li, Y., Cui, H., Chen, L., Li, H., Zou, Y., Long, C., Lan, L., Chai, J., et al. (2007). A *Pseudomonas syringae* effector inactivates MAPKs to suppress PAMP-induced immunity in plants. Cell Host Microbe *1*, 175–185.

Zipfel, C., Kunze, G., Chinchilla, D., Caniard, A., Jones, J.D.G., Boller, T., and Felix, G. (2006). Perception of the bacterial PAMP EF-Tu by the receptor EFR restricts *Agrobacterium*-mediated transformation. Cell *125*, 749–760.

ISCI, Volume *3*

Supplemental Information

Leptosphaeria maculans Effector Protein AvrLm1 Modulates Plant Immunity by Enhancing MAP Kinase 9 Phosphorylation

Lisong Ma, Mohammad Djavaheri, Haiyan Wang, Nicholas J. Larkan, Parham Haddadi, Elena Beynon, Gordon Gropp, and M. Hossein Borhan

Supplemental Information

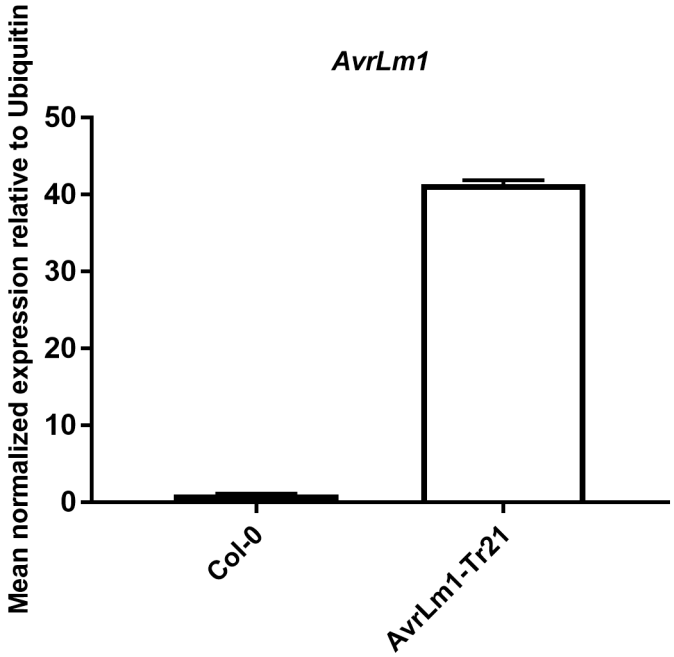

Figure S1. Related to figures 1 and 2. qPCR showing *AvrLm1* expression in *AvrLm1*-overexpressing Arabidopsis line. *AvrLm1* gene expression level was normalized to Arabidopsis gene *Ubiquitin*. Values represent means ± standard error (SE) from three independent experiments.

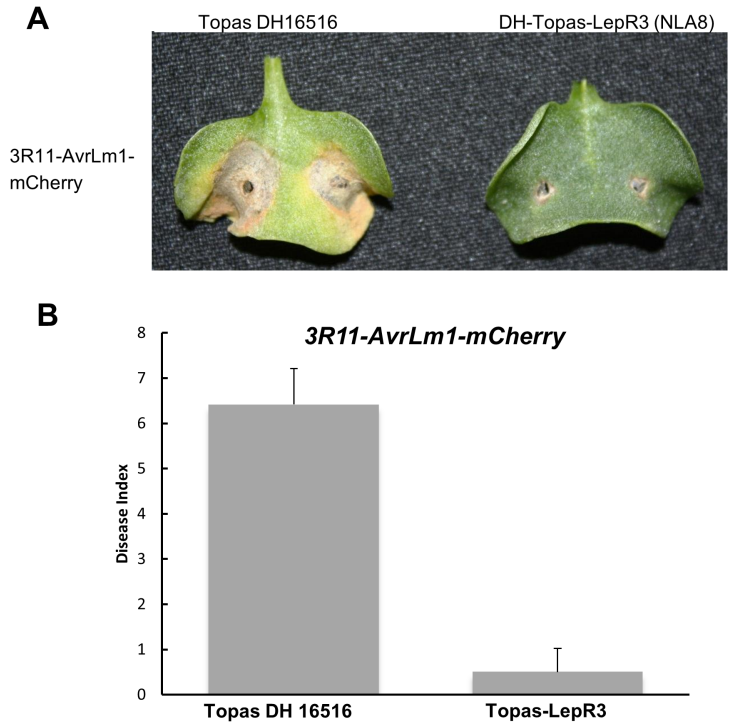

Figure S2. Related to figure 3. *L. maculans* 3R11-AvrLm1-mCherry causes disease on susceptible Topas DH16516, but not on Topas:LepR3 plants. Cotyledons of 7-day-old seedlings of susceptible *B. napus* Topas DH16516 and Topas:LepR3 (NLA8) lines were inoculated with a transgenic *L. maculans* 3R11 isolate carrying AvrLm1-mCherry. **A)**. Images were taken from infected cotyledons of seedlings 10 days after inoculation. **B)**. Average disease index representing data collected from 12 cotyledons of susceptible Topas DH16516 and Topas:LepR3 transgenic plants (NLA8).

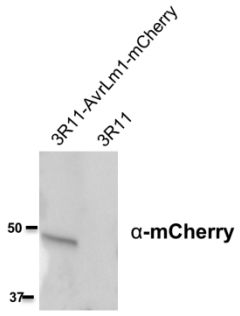

Figure S3. Related to figure 3. AvrLm1-mCherry fusion protein is detected from apoplastic fluids isolated from cotyledons infected with *L. maculans* 3R11 carrying *AvrLm1-mCherry*. Cotyledons of 7-day-old seedlings of susceptible *B. napus* Topas DH16516 were inoculated with a transgenic *L. maculans* 3R11 isolate carrying *AvrLm1-mCherry* or 3R11. Apoplastic fluids isolated from cotyledons 4 days after inoculation were concentrated and probed with anti-mCherry antibody and expected protein band with molecular weight 48 KDa was detected.

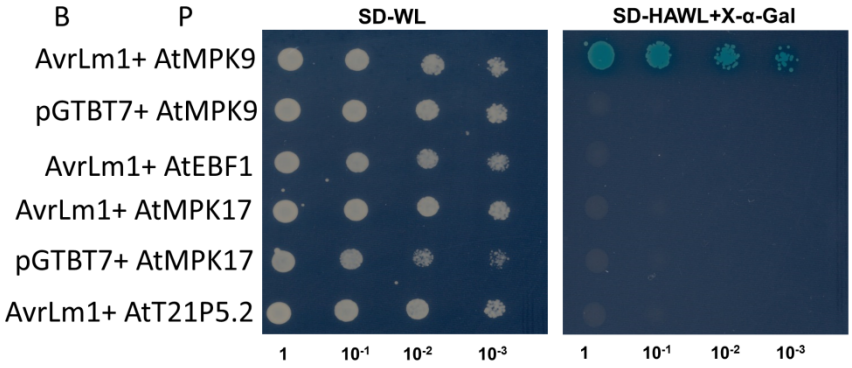

Figure S4. Related to figure 4. Testing the interaction of AvrLm1 with full length of candidate genes obtained from yeast two hybrid screening. Four candidate genes as prey (P) including *AtEBF1*, *AtMPK9*, *AtMPK17* and *AtT21P5.2* were co-transformed with *AvrLm1* as bait (B) or empty vector to yeast, respectively. All transformants were able to grow on SD-WL medium. Yeast were able to grow on selective medium (SD-HAWL+X-α-Gal) with development of blue coloration indicating a protein-protein interaction. Representative pictures were photographed 3 days after incubation at 30 °C.

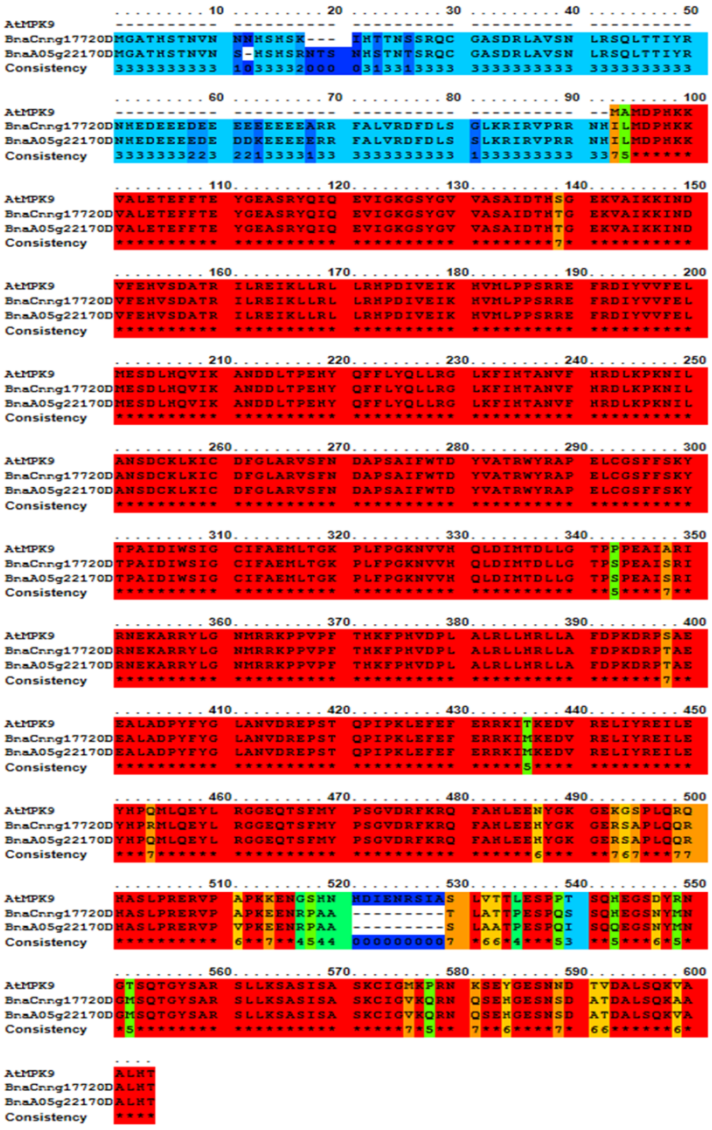

Figure S5. Related to figure 4. Protein sequences alignment between AtMPK9 and the two homologous ones from *B. napus*.

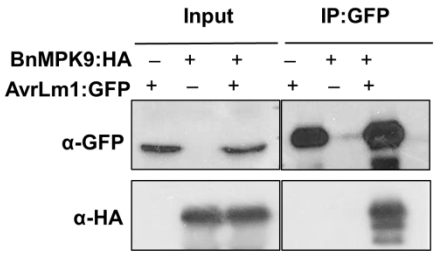

Figure S6. **Related to figure 4**. **Avrlm1 associates with BnMPK9.** Co-immunoprecipitation of AvrLm1 and BnMPK9 from total plant protein extracts. GFP-tagged *AvrLm1* and HA-tagged BnMPK9 were co-expressed in *N. benthamiana*. Proteins were extracted after 48 h and subjected to immunoprecipitation by GFP-Trap beads. Immunoprecipitated proteins (IPs) were analysed by immunoblotting by probing with either anti-HA (α-HA) or anti-GFP (α-GFP).

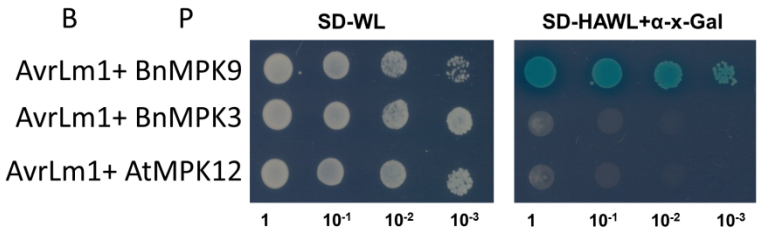

Figure S7. **Related to figure 4**. **AvrLm1 specifically interacts with BnMPK9.** Arabidopsis *MPK12* (*AtMPK12*) or *B. napus MPK3* (*BnMPK3*) or *BnMPK9* was co-transformed with *AvrLm1* to yeast. There were no interactions between AvrLm1 and AtMPK12 or BnMPK3.

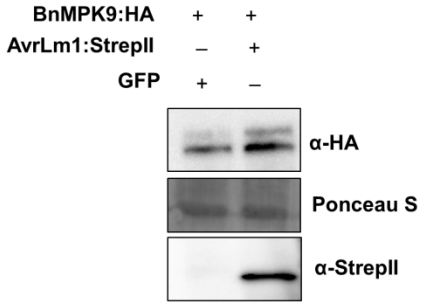

Figure S8. Related to figure 7. **AvrLm1 is able to stabilize the accumulation of BnMPK9 *in planta***. Western blot probed with anti-HA and anti-StrepII antibodies showing the stabilization of BnMPK9 in the presence of AvrLm1 in transient expression. HA-tagged *BnMPK9* was co-expressed with StrepII-tagged *AvrLm1* or *GFP* in *N. benthamiana* leaves using agroinfiltration. Proteins were extracted after 48 h post infiltration and subjected to western blotting.

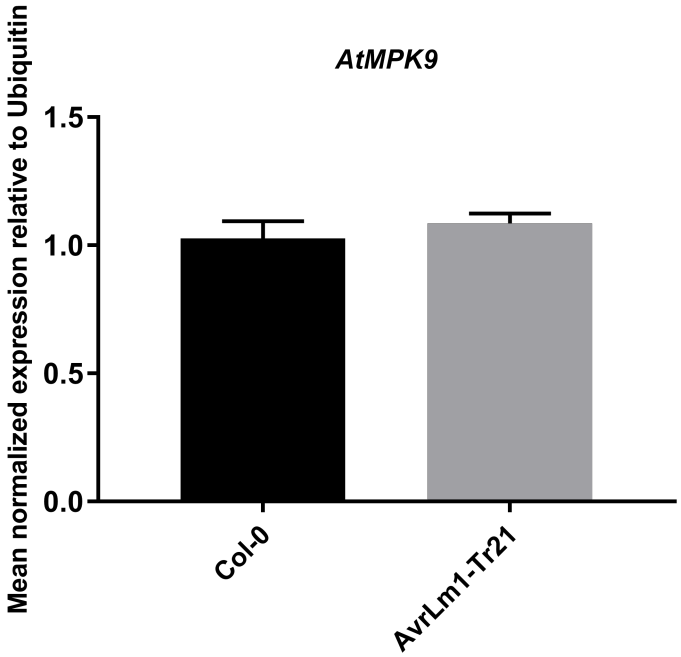

Figure S9. Related to figure 7. qPCR showing *AtMPK9* expression in *AvrLm1*-overexpressing Arabidopsis lines. *AtMPK9* gene expression levels are normalized to Arabidopsis Ubiquitin gene. Values represent means ± standard error (SE) from three independent experiments.

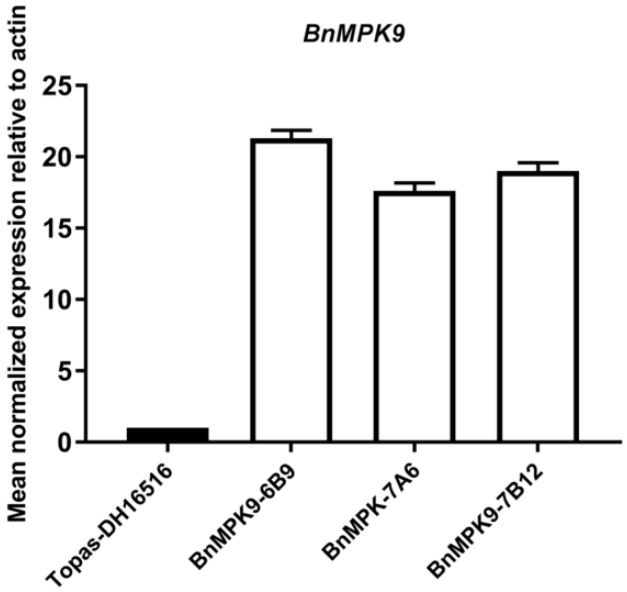

Figure S10. Related to figures 8, 9 and 10. qPCR showing *BnMPK9* expression in *BnMPK9*-overexpressing *B. napus* lines. *BnMPK9* gene expression levels are normalized to *B. napus* actin gene. Values represent means ± standard error (SE) from three independent experiments.

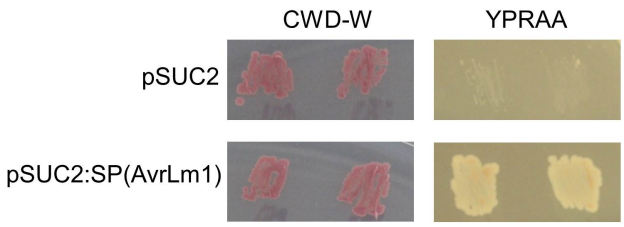

Figure S11. Related to figures 3 and S3. Yeast signal sequence trap assay of the predicted signal peptide of AvrLm1 protein. The predicted signal peptide sequences plus the following two amino acids (1–24) of AvrLm1 and the negative control pSUC2 vector were used for the assay. CMD-W (minus Trp) plates were used to select yeast strain YTK12 carrying the pSUC2 vector. Sucrose and YPRAA media were used to indicate invertase secretion.

Table S1. Related to figure 4. Arabidopsis candidates from yeast two-hybrid screening.

Gene names	Accession number	Independent clones
Arabidopsis thaliana EBF1 (EIN3-BINDING F BOX PROTEIN 1)	AT2G25490.1	28
Arabidopsis thaliana - MPK17	AT2G01450.1	32
Arabidopsis thaliana - MPK9	AT3G18040.1	30
Arabidopsis thaliana - T21P5.2 (hypothetical protein)	AT3G03560.1	18

Table S2. Primers used in this study

Primer names	Sequences
BnMPK9-FB	ACAAGTTTGTACAAAAAAGCAGGCTTCATGGGTGCTACTCACAGCACCAAC
BnMPK9-RB	ACCACTTTGTACAAGAAAGCTGGGTCTCAAGTGTGGAGAGCCGCGGCCTTTT
YFP-FB	ACAAGTTTGTACAAAAAAGCAGGCTTCATGGTGAGCAAGGGCGAGGAGCTGTT
YFP-RB	ACCACTTTGTACAAGAAAGCTGGGTCTTATCCGGTGGATCCCGGGCCCG
BnMPK9-NdeI	GCGGCATATGATGGGTGCTACTCACAGCACCAAC
BnMPK9-KD-FB	ACAAGTTTGTACAAAAAAGCAGGCTTTACTAGTGATGAGTCGGTATCAGATCCAAG AAGTTA
BnMPK9-KD-RB	ACCACTTTGTACAAGAAAGCTGGGTCACTAGTAAAGTAAGGATCTGCCAGTGCCT
BnMPK9-EcoRI	GCGGGAATTCTCAAGTGTGGAGAGCCGCGG
BnMPK9-KD-EcoRI	GCGGGAATTCTCAAAAGTAAGGATCTGCCAGTGCCTCT
BnMPK9-N-KD-NdeI	GCGGCATATGATGTATGGACTGGCAAACGTGGATCG
AvrLm1-FB	ACAAGTTTGTACAAAAAAGCAGGCTTTATGGTTCAATTCAAGACTATCTTTCTATCA
ΔspAvrLm1-FB	ACAAGTTTGTACAAAAAAGCAGGCTTTATGTCCCCAGCTACCAAGAACAATGTGA
AvrLm1-RB-S	ACCACTTTGTACAAGAAAGCTGGGTCTATTGCACCCGCAATATCAAATTTT
AtEBF1-NdeI	GCGGCATATGTCTCAGATCTTTAGTTTTGCCGG
AtEBF1-EcoRI	GCGGGAATTCTCAGGAGAGGATGTCACATTTGTAAAG
AtMPK17-NdeI	GCGGCATATGTTGGAGAAAGAGTTTTTCACGGA
AtMPK17-XhoI	ACGCCTCGAGCTATGACACTGCAGAGGAGACACCAA
AtT21P5.2-NdeI	GCGGCATATGGATCATGATCACATGCATGGAA
AtT21P5.2-EcoRI	GCGGGAATTCTCAACAAGCACAACCTGAGGGAGGA
AtMPK12-EcoRI	GCGGGAATTCATGTCTGGAGAATCAAGCTCTGGTTCT
AtMPK12-XhoI	ACGCCTCGAGTCAGTGGTCAGGATTGAATTTGACA
BnMPK3-EcoRI	GCGGGAATTCATGAACAACGCCGGCGGCCA
BnMPK3-XhoI	ACGCCTCGAGCTAAGCATATGTTGGATTGAGTGCAATGGC
ΔspAvrLm1-NdeI	GCGGCATATGATGTCCCCAGCTACCAAGAACAATGTG
ΔspAvrLm1-EcoRI	GCGGGAATTCTTACTTCTCGAATTGTGGGTGGCT
AvrLm1ND1-NdeI	GCGGCATATGGATAATACTGAAAATAACCACAACCTGGAG
AvrLm1ND1-EcoRI	GCGGGAATTCTTACTTCTCGAATTGTGGGTGGCT
AvrLm1ND2-NdeI	GCGGCATATGATGGCCTGGCTGATAGACTTCAGC
AvrLm1ND3-NdeI	GCGGCATATGGATGTCGTGGTTCCGCTCATTAC
AvrLM1CD1-EcoRI	GCGGGAATTCTTATATTGCACCCGCAATATCAAATTTTA
BnActin-Q-F	CTGGAATTGCTGACCGTATGAG
BnActin-Q-R	ATCTGTTGGAAAGTGCTGAGGG
BnMPK9-Q-F	CCTCAGAGTTCTCAACACGAG
BnMPK9-Q-R	CTGGTTCCTTTGTTTCACGC
BnPR1-Q-F	CATCCCTCGAAAGCTCAAGAC
BnPR1-Q-R	CCACTGCACGGGACCTAC
BnWRKY70-Q-F	ACATACATAGGAAACCACACG
BnWRKY70-Q-R	ACTTGGACTATCTTCAGAATGC
BnAOS-Q-F	CGCCACCAAAACAACAAAG
BnAOS-Q-R	GGGAGGAAGGAGAGAGGTTG
BnLOX3-Q-F	GAAGTTTATGGCGGTGGT
BnLOX3-Q-R	CCTGTTTCTACGGTTAGGA
AtUbiquitin-Q-F	GCTCTTATCAAAGGACCTTCGG
AtUbiquitin-Q-R	CGAACTTGAGGAGGTTGCAAAG
AtPR1-Q-F	CGTCTTTGTAGCTCTTGTAGGTGC
AtPR1-Q-R	TGCCTGGTTGTGAACCCTTAG
AtLOX2-Q-F	ATCAACAAGCCCCAATGGAA
AtLOX2-Q-R	CGGCGTCATGAGAGATAGCAT
AtPR4-Q-F	AGCTTCTTGCGGCAAGTGTTT
AtPR4-Q-R	TGCTACATCCAAATCCAAGCCT
AtABF2-Q-F	AGAGAATGACGAGTTACAACGAAAG

AtABF2-Q-R	TAAAACACCTAAGTGGGATGTCATT
SP-AvrLm1-F	CGGCGGAATTCATGGTTCAATTCAAGACTATCTTTCTATCA
SP-AvrLm1-R	GCCGCCTCGAGAGCTGGGGAGCTAGAACCTGTT
AtMPK9-q-F1	GCCAGCATCAGTGCATCTA
At-MPK9-q-R1	GAGACAGAGCATCAACCGTATC

Transparent methods

Plant growth and infection conditions

The susceptible doubled-haploid (DH) *B. napus* cv. Topas DH16516, NLA8-2 (Topas: *LepR3*) and single-spore cultures of the *L. maculans* isolates v23.1.3 and 3R11 were used in this study. Plant growth and *L. maculans* infection conditions were described previously (Larkan et al., 2014). Briefly, seedlings were grown in a growth chamber at 20°C, 16 h days, and light intensity c. 450 µmol m^{-2} s^{-1} at bench level, and 18°C, 8 h nights. Pycnidiospore inoculum, (10 µL of 2×10^7 spores/mL suspensions) was placed on the wounded site of a cotyledon of 7-day-old seedlings (4 infection sites per seedling). After inoculation, the seedlings were kept in the same growth condition as described above.

Generation of transgenic *L. maculans* strains

AvrLm1-mCherry insert DNA with Gateway attB linkers was synthesized (GenScript, USA) and recombined into the Gateway entry clone pDONR/Zeo and then into the destination binary vector GW-pLM4 (Ma and Borhan, 2015) as instructed by the manufacture (Invitrogen) resulting in the plasmid pLM4::*AvrLm1-mCherry*. The YFP gene was amplified with the primer set YFP-FB/YFP-RB using pEarlyGate101 as a template. YFP fragment was first recombined into the entry clone pDONR/Zeo and then into the binary vector pJU472 (Utermark and Borhan, unpublished) to obtain pJU472::*YFP* construct. pLM4::*AvrLm1-mCherry* and pJU472::*YFP* were transformed into Agrobacterium AGL1 and used for subsequent *Agrobacterium tumefaciens*-mediated transformation of pycnidospores from the *L. maculans* isolate '3R11' (*avrLm1*), as described by (Utermark and Karlovsky, 2008).

Binary vector constructions

For stable plant transformation, the *Brassica napus MPK9* (*BnMPK9*) ORF was amplified using primers BnMPK9-FB and BnMPK9-RB (Table S2) from the *L. maculans-B. napus* cDNA library. The PCR product was introduced into entry clone pDONR/Zeo (Invitrogen) and then into the binary vector pEarlyGate100 (Earley et al., 2006). At the same time, the *AvrLm1* coding sequences with or without signal peptide plus AttB gateway linker and C-terminal StrepII tag was synthesized (GenScript). The resulting plasmid pUC57:*AvrLm1* and pUC:Δsp*AvrLm1* were recombined, via entry vector pDONR/Zeo, followed by recombination into destination vector pEarlyGate100. pEarlyGate100:*BnMPK9,* pEarlyGate100:*AvrLm1-StrepII and* pEarlyGate100:Δsp*AvrLm1-StrepII* were used for agrotransformation.

For transient expression, full length *AvrLm1* was PCR-amplified from *L. maculans-B. napus* cDNA library using primers AvrLm1-FB and AvrLm1-RB. The truncated *AvrLm1* lacking the signal peptide sequence was amplified using primers ΔspAvrLm1-FB and AvrLm1-RB. The PCR products were introduced into entry clone pDONR/Zeo (Invitrogen) to obtain

pENTR/Zeo:*AvrLm1* and pENTR/Zeo:Δsp*AvrLm1*. The kinase domain of *BnMK9* was amplified with primer set BnMPK9-KD-FB/BnMPK9-KD-RB. pENTR/Zeo:*AvrLm1* and pENTR/Zeo:Δsp*AvrLm1* were recombined into the binary vector pEarlyGate100. The *BnMPK9* insert encoding the protein with mutated TDY motif was synthesized (GenScript). pUC57:*BnMPK9mTDY* was recombined via entry vector pDONR/Zeo into pEarlyGate100. The resulting plasmids pEarlyGate100:*AvrLm1,* pEarlyGate100:*BnMPK9-KD*, pEarlyGate100:Δsp*AvrLm1* and pEarlyGate100: *BnMPK9mTDY* were used for *Agrobacterium*-mediated transformation and transient assay.

To generate the BiFC constructs, pENTR/Zeo:*BnMPK9* and pENTR/Zeo:Δ*spAvrLm1* were recombined into the binary vectors pDEST-GW-VYCE and pDEST-GW-VYNE, respectively (Gehl et al., 2009). The resulting plasmids pDEST:*BnMPK9-VYCE*, pDEST:*BnMPK9-VYNE* and pDEST: Δ*spAvrLm1-VYNE* were used for *Agrobacterium* transformation.

For co-immunopreipication, the pENTR/Zeo:Δ*spAvrLm1* was recombined into the binary vector pGWB451 containing the C-terminal GFP (Nakagawa et al., 2007), which resulted in the pGWB451:Δsp*AvrLm1*. pENTR/Zeo:*BnMPK9* was recombined into binary vector pEarlyGate201 containing the N-terminal HA tag fused to MPK9. All pDONR/Zeo clones were confirmed by sequencing. All resulting binary plasmids were transformed to *A. tumefaciens* strain GV3101 (pMP90). *Agrobacterium*-mediated transient expression in *N. benthamiana* was performed according to methods described previously (Ma et al., 2012).

For the yeast two-hybrid, *AvrLm1* lacking signal peptide sequencing was cloned into pGBKT7 bait vector with primer set ΔspAvrLm1-NdeI/ΔspAvrLm1-EcoRI and the *BnMPK9* was cloned into pGADT7 prey vector with primer set BnMPK9-NdeI/BnMPK9-EcoRI (Clontech). The *Brassica napus MPK3* (*BnMPK3*), *AtMPK12*, *AtMPK17*, *AtEBF1*, *AtMPK9* and *AtT21P5.2* ORFs were amplified using primers listed in Table S2 from *L. maculans*-*B. napus* cDNA library or Arabidopsis cDNA. Series of truncated *ΔspAvrLm1* and *BnMPK9* were amplified using the primers listed in Table S2. The PCR products were cloned into pGADT7 (Clontech, Mountain View, USA).

For yeast signal sequence trap experiment, the signal peptide fragment of *AvrLm1* gene was obtained via PCR. The amplification was performed with primer pair SP-AvrLm1-F/SP-AvrLm1-R using pENTR/Zeo:AvrLm1 as a template. The obtained product, carrying *Eco*RI and *Xho*I restriction sites, was cloned into the vector pSUC2 digested with the same restriction enzymes.

Plant transformation

Arabidopsis thaliana ecotype Columbia (Col) was transformed by the floral dip method (Clough and Bent, 1998). First-generation transformations were selected with herbicide BASTA. Several independent homozygous single insertion lines were selected based on segregation analyses and homozygous T4 lines were used for further experiments. Transformation of *B. napus* Topas DH16516 with pEarlyGate100:*BnMPK9* construct was conducted as described by De Block *et al*. (De Block et al., 1989).

Yeast two hybrid library screening and assays

Initial screening of *A. thaliana* cDNA library was performed by Hybergenics (France) using ULTImate Y2H. *AvrLm1* lacking signal peptide sequence was cloned into pB27 vector as the bait.

To confirm the potential target genes identified after the first round of screening we used the matchmaker GLA4 two-hybrid system and yeast strain Y2HGold (Clontech, Mountain View, USA). The yeast strain Y2HGold was co-transformed with bait and prey plasmid combinations using lithium-acetate and polyethylene glycol 3350 as described previously (Daniel Gietz and Woods, 2002). Transformants harboring both bait and prey plasmids were selected on plates containing minimal medium lacking Leu and Trp (SD-WL). Empty prey vector pGBKT7 or pGADT7 used as bait or prey served as controls. One colony per combination was picked from SD-WL plates to inoculate 1 mL SD-WL culture. After 36 h growth, cells were collected by centrifugation and resuspended in 25 µL 0.9% NaCl from OD_{600}=1 to OD_{600}=0.00001 and spotted on SD-WL and SD-AHWL plates supplementing with 40 µg/mL X-α-Gal (Clontech, Mountain View, USA) and 200 ng/ml Aureobasidin A (Clontech, Mountain View, USA). After 3 days incubation, the plates were checked for growth and photographed.

RNA isolation and quantitative PCR

Cotyledons discs (2mm in diameter) from 10-day-old Topas DH16516 and Topas:*BnMPK9* seedlings were collected, frozen in liquid nitrogen and stored at −80 °C. Leaves of 4 to 5-weeks-old Arabidopsis plants were collected and immediately frozen in liquid nitrogen, and stored at −80 °C prior to extraction of total RNA. Total RNA from the samples was extracted with TRIzol LS reagent (Invitrogen) and subsequently purified with RNeasy Mini kit (Qiagen). DNA was removed by on-column treatment with RNase-free DNase (Qiagen). qRT-PCR was performed using a CFX96 qPCR machine (Bio-Rad) and SsoAdvanced™ Universal SYBR® Green Supermix (BIO-RAD). RT-PCR was performed for all tested *genes* with three biological samples. The primers used for qRT-PCR are described in Table S2. *Ct* values were analysed according to the $2^{-\Delta\Delta Ct}$ method (Livak and Schmittgen, 2001). The *B. napus* actin and Arabidopsis ubiquitin served as reference genes. The statistical significance of differences was calculated using GraphPad Prism 6 (GraphPad Software, Inc., USA) with one-way ANOVA followed by the Turkey post-test or with the two-tailed Student's *t*-test to obtain the P-value. Data are shown as mean ± SEM of three biological replicates from one representative experiment. Significant differences between treatments and controls are represented by three ($P < 0.001$), two ($p<0.01$) or one asterisk ($p<0.05$).

Bimolecular fluorescence complementation

For BiFC assays, infiltration was done on the leaves of 4- to 5-week-old *N. benthamiana* plants with Agrobacteria containing the corresponding constructs at an absorbance density of 0.5. Leaf discs 48 h after infiltration were imaged. Confocal microscopical analysis was performed with the LSM610 (Zeiss, Germany). Excitation of the mCherry was detected at 543 nm with HeNe laser. The 590-610 nm filter captured emission.

Apoplastic fluids isolation

Cotyledons of 7-day-old Topas DH16516 were inoculated with *L. maculans* isolate 3R11(naturally lacks *AvrLm1*) transformed with *AvrLm1-mCherry* or wild type 3R11 4-day-after inoculation, 96 cotyledons were collected for each inoculum and the apoplastic fluids (AF) were

isolated according to the previously descried method (Joosten, 2012). Briefly, collected cotyledons were placed in a beaker filled with deionised water and a weight was placed on the top of cotyledons. Next, a vacuum was applied with a final pressure of about 60 mbar (hPa). The infiltrated cotyledons were centrifuged at 1000 *g* for 10 min at 4°C. After centrifugation, the obtained AF was concentrated with Amicon® Ultra (Millipore) unit to a final volume of 200-300 µL Concentrated AF was used for immunoblotting with monoclonal anti-mCherry antibody (Sigma) at a dilution 1:2000.

Protein extraction

Protein from agroinfiltrated leaves was extracted as described previously (Ma et al., 2013; Liebrand et al., 2013). Briefly, the total protein fractions were extracted from *N. benthamiana* leaves 48 h after infiltrating with mixture of *A. tumefaciens* GV3101 containing either pEarlyGate201:*BnMPK9* and *GFP* or pEarlyGate100::Δsp*AvrLm1-StrepII* and pEarlyGate201::*BnMPK9* in the presence or absence of 26S proteasome inhibitor MG132 (100mM) and DMSO, which was infiltrated into the leaves at 24 h after agroinfiltration. The frozen leaves were ground in liquid nitrogen and suspended in 1 ml protein extraction buffer per gram of tissue (25 mM Tris, pH 8, 1 mM EDTA, 5 mM DTT, 150 mM NaCl, 0.1% IGEPAL CA-630 [NP-40], 1x Roche complete protease inhibitor cocktail and 2% PVPP). Extracts were centrifuged at 12,000 g at 4°C for 10 min, and the supernatant was passed over four layers of Miracloth to obtain a total protein lysate. After running the SDS-PAGE gels, the samples were blotted on PVDF membranes using semi-dry blotting. Skimmed milk powder (5%) was used as blocking agent (PBS, 0.1% Tween 20).

Co-immunoprecipitation

Co-IP was performed as previously described (Ma et al., 2013). Briefly, the total protein fractions were extracted from *N. benthamiana* leaves 48 h after infiltrating with mixture of *A. tumefaciens* GV3101 containing either pEarlyGate201:*BnMPK9* and *GFP* or pGWB451:Δsp*AvrLm1* and pEarlyGate201::*BnMPK9*. Extracts were centrifuged at 12,000 g for 15 min, and 1 ml supernatant was added to 50 µL of HA-tag beads (Roche) or GFP-Trap (ChromoTek) , which was incubated for 1.5 h at 4 °C in a rotator. After washing the beads four times with extraction buffer, immunoprecipitated proteins were separated by 8% SDS-PAGE gels and blotted onto PVDF membrane (Bio-Rad) overnight using wet blotting. Skimmed milk powder (5%) was used as blocking agent. A 1:1000 dilution of anti-GFP antibody (Sigma) or 1:8000 diluted anti-HA-HRP (Pierce) was used. The secondary antibody goat-anti-mouse (Pierce) was used as a 1:15000 dilution. The luminescent signal was visualized by Immobilon Western Chemiluminescent HRP Substrate using Bio-Rad ChemiDoc imager (Bio-Rad).

To isolate BnMPK9 for MPK phosphorylation assays, 2 mL protein lysate was incubated for 2 hr with 3 mg anti-MPK9 antibodies at 4 °C followed by incubation for 1 hr with 50 µL Goat-anti mouse magnetic beads (NEB). After washing the beads four times with the extraction buffer, proteins were eluted by boiling in 60 mL Laemmli loading buffer. Immunoprecipitated proteins were separated by 8% SDS-PAGE gels and blotted onto PVDF membrane (Bio-Rad) using wet blotting for overnight. BSA (5%) was used as blocking agent. A 1:8000 dilution of anti-HA-HRP (Pierce) and 1:1000 dilution of monoclonal anti-Phosphothreonine antibody (Sigma) were used. The secondary antibody goat-anti-mouse (Pierce) was used as a 1:15000 dilution. The

luminescent signal was visualized by Immobilon Western Chemiluminescent HRP Substrate using Bio-Rad ChemiDoc imager (Bio-Rad).

***Pseudomonas syringae* infection assays in Arabidopsis**

The *Pseudomonas syringae* infection assays in Arabidopsis was performed as described previously (Yao et al., 2013). The virulent strain of *Pst* DC3000 was used in this study. Bacterial cells were grown overnight in King's B medium broth at 28°C. Leaves of the 5-week-old plants were syringe inoculated with a bacterial suspension of *Pst* DC3000 [1×10^8 colony-forming units (cfu) mL^{-1}] in 10 mM $MgCl_2$ containing 0.02% Silwet L-77. The inoculated plants were kept at 100% humidity for 24 h and then raised in a growth chamber under the same condition as described above. Bacterial growth in the infected leaves of each plant was determined according to the previously described method (Van Poecke et al., 2007). Three days after inoculation, two leaf discs (total surface 0.57 cm^2) were punched from a single leaf using a new plant for each time point. Leaf discs were pulverized in 400 µL 5 mM $MgSO_4$, and a dilution series of the suspension was made. Of each dilution, 10 µL was streaked on King's B plates containing appropriate antibiotics. After 2 d, colonies were counted from the dilution that resulted in 15 to 150 colonies per streak. From this data, the $\log_{10}$ of the number of cfu per cm^2 leaf surface was calculated. The experiment was repeated three times, with eight replicates per genotype per treatment in each experiment.

Quantification of *L. maculans* in cotyledons of *B. napus*

Quantification of *L. maculans* in inoculated infected cotyledons of *B. napus* was conducted according to the method described previously (Sasek et al., 2012). DNA was extracted from cotyledons using hexadecyltrimethylammonium bromide (CTAB) based method. DNA (100 ng) was used as a template for a qPCR performed with *LmITS1* and *BnActin* primers and the following program: 95°C for 10 min; followed by 45 cycles of 95°C for 10 s, 55°C for 10 s, and 72°C for 10 s; followed by a melting curve analysis. The relative quantity of *LmITS1* was normalized to *B. napus Actin*. The statistical significance of differences was calculated using GraphPad Prism 6 (GraphPad Software, Inc., USA) with one-way ANOVA to obtain the P-value. Data are shown as mean ± SEM of three biological replicates from one representative experiment. Significant differences between treatments and controls are represented by three ($P < 0.001$), two ($p<0.01$) or one asterisk ($p<0.05$).

DAB staining to detect hydrogen peroxide

3,3-Diaminobenzidine (DAB) stainging was conducted following the protocls described previoulsy (Sasek et al., 2012). Briefly, DAB solution was prepared by dissolving 30 mg of DAB (Sigma-Aldrich) in 150 µl of dimethylformamide and mixing it with 30 ml of water. Six detached cotyledons collected from individual plants without inoculation of *L. maculans* or four-day post inoculation were immersed in the staining solution and infiltrated under vacuum. Subsequently, cotyledons were kept at room temperature in a closed petri dish in darkness until reddish-brown staining was visualized. After that, cotyledons were destained in 96% ethanol to remove Chlorophyll. Next, cotyledons were rehydrated in water and scanned in a reflective mode.

Yeast signal sequence trap system

Yeast transformation was performed according to the protocol listed in the YeastmakerTM Yeast Transformation System 2 (Clontech, USA). The invertase negative yeast strain YTK12 was transformed with 20 ng of the pSUC2:*SP(AvrLm1)* or empty vector pSUC2. After transformation,

yeast was plated on CMD-W (minus Trp) plates (0.67% yeast N base without amino acids, 0.075% W dropout supplement, 2% sucrose, 0.1% glucose, and 2% agar). Transformed colonies were transferred to fresh CMD-W plates and incubated at 30°C for 3 days. For the invertase secretion assay, transformed colonies were replica plated on CMD-W plates and YPRAA plates (1% yeast extract, 2% peptone, 2% raffinose, and 2 μg/mL antimicyn A) containing raffinose and lacking glucose. After 3 days incubation at 30 °C, the plates were checked for growth and photographed.

Data and Software Availability

AvrLm1 yeast-two hybrid screening candidates using Arabidopsis cDNA library with Arabidopsis accession number: AT2G25490.1, AT2G01450.1, AT3G18040.1 and AT3G03560.1

Supplemental References

Clough, S.J., and Bent, A.F. (1998). Floral dip: a simplified method for *Agrobacterium*-mediated transformation ofArabidopsis thaliana. Plant J. *16*,735-743.

Daniel Gietz, R., and Woods, R.A. (2002). Transformation of yeast by lithium acetate/single-stranded carrier DNA/polyethylene glycol method. In Methods in Enzymology, G. Christine, and R.F. Gerald, eds. (Academic Press), pp. 87-96.

De Block, M., De Brouwer, D., and Tenning, P. (1989). Transformation of *Brassica napus* and *Brassica oleracea* using *Agrobacterium tumefaciens* and the expression of the bar and neo genes in the transgenic plants. Plant physiol. *91*, 694-701.

Earley, K.W., Haag, J.R., Pontes, O., Opper, K., Juehne, T., Song, K., and Pikaard, C.S. (2006). Gateway-compatible vectors for plant functional genomics and proteomics. Plant J. *45*, 616-629.

Gehl, C., Waadt, R., Kudla, J., Mendel, R.R., and Hansch, R. (2009). New GATEWAY vectors for high throughput analyses of protein-protein interactions by bimolecular fluorescence complementation. Mol Plant. *2*, 1051-1058.

Larkan, N., Lydiate, D., Yu, F., Rimmer, S., and Borhan, M. (2014). Co-localisation of the blackleg resistance genes *Rlm2* and *LepR3* on Brassica napus chromosome A10. BMC Plant Biol. *14*, 1-9.

Liebrand, T.W., van den Berg, G.C., Zhang, Z., Smit, P., Cordewener, J.H., America, A.H., Sklenar, J., Jones, A.M., Tameling, W.I., Robatzek, S.*, et al.* (2013). Receptor-like kinase SOBIR1/EVR interacts with receptor-like proteins in plant immunity against fungal infection. Proc. Natl. Acad. Sci. U S A. *110*, 10010-10015.

Livak, K.J., and Schmittgen, T.D. (2001). Analysis of relative gene expression data using real-time quantitative PCR and the 2−ΔΔCT method. Methods *25*, 402-408.

Ma, L., Lukasik, E., Gawehns, F., and Takken, F.L. (2012). The use of agroinfiltration for transient expression of plant resistance and fungal effector proteins in Nicotiana benthamiana leaves. Methods Mol. Biol. *835*, 61-74.

Ma, L., Cornelissen, B.J.C., and Takken, F.L.W. (2013). A nuclear localization for Avr2 from *Fusarium oxysporum* is required to activate the tomato resistance protein I-2. Front. Plant Sci. *4*.

Nakagawa, T., Suzuki, T., Murata, S., Nakamura, S., Hino, T., Maeo, K., Tabata, R., Kawai, T., Tanaka, K., Niwa, Y., *et al.* (2007). Improved Gateway binary vectors: high-performance vectors for creation of fusion constructs in transgenic analysis of plants. Biosci. Biotechnol. Biochem. *71*,2095-2100.

Joosten, M.H.A.J. (2012). Isolation of apoplastic fluid from feaf tissue by the vacuum infiltration-centrifugation technique. In Plant Fungal Pathogens: Methods and Protocols, M.D. Bolton, and B.P.H.J. Thomma, eds. (Totowa, NJ, Humana Press), pp. 603-610.

Sasek, V., Novakova, M., Jindrichova, B., Boka, K., Valentova, O., and Burketova, L. (2012). Recognition of avirulence gene AvrLm1 from hemibiotrophic ascomycete *Leptosphaeria maculans* triggers salicylic acid and ethylene signaling in *Brassica napus*. Mol. Plant Microbe Interact. *25*, 1238-1250.

Utermark, J., and Karlovsky, P. (2008). Genetic transformation of filamentous fungi by *Agrobacterium tumefaciens*. doi:10.1038/nprot.2008.83.

Van Poecke, R.M.P., Sato, M., Lenarz-Wyatt, L., Weisberg, S., and Katagiri, F. (2007). Natural variation in RPS2-mediated resistance among Arabidopsis accessions: correlation between gene expression profiles and phenotypic responses. Plant Cell. *19*, 4046-4060.

Yao, J., Withers, J., and He, S.Y. (2013). *Pseudomonas syringae* infection assays in Arabidopsis. Methods Mol. Biol. *1011*, 63-81.